CHALMERS
UNIVERSITY OF TECHNOLOGY

A sequential-adaptive strategy in space-time with application to consolidation of porous media

Available online at www.sciencedirect.com
ScienceDirect
Comput. Methods Appl. Mech. Engrg. 288 (2015) 146–171
Computer methods in applied mechanics and engineering
www.elsevier.com/locate/cma

A sequential-adaptive strategy in space–time with application to consolidation of porous media

Fredrik Larsson*, Kenneth Runesson

Department of Applied Mechanics, Chalmers University of Technology, S-41296 Göteborg, Sweden

Available online 10 December 2014

Highlights

- A novel approach for space–time adaptive finite element analysis is presented.
- Global error control is obtained by the technique of solving a dual problem.
- Space and time errors are estimated using a hierarchical decomposition of the dual.
- Recursive adaptations of the whole space–time mesh is avoided.
- The coupled consolidation problem in geomechanics is considered as an application.

Abstract

Issues related to space–time adaptivity for a class of nonlinear and time-dependent problems are discussed. The dG(k)-methods are adopted for the time integration, and the a posteriori error control is based on the appropriate dual problem in space–time. One key ingredient is to decouple the error generation in space and time with a hierarchical decomposition of the discrete space of dual solutions. The main idea put forward in the paper is to increase the computational efficiency of the adaptive scheme by avoiding recursive adaptations of the whole time-mesh; rather, the space-mesh and the time-step defining each finite space–time slab are defined in a truly sequential fashion.

The proposed adaptive strategy is applied to the coupled consolidation problem in geomechanics involving large deformations. Its performance is investigated with the aid of a numerical example in 2D.

Keywords: Adaptivity; Error estimate; Finite element analysis; Porous media

1. Introduction

One of the classical coupled field problems in continuum mechanics is the time-dependent deformation of a porous medium, when the pores are (partly) filled with a fluid, cf. de Boer [1]. In soil mechanics, this is denoted the consolidation problem (pertinent to fine-grained soils like clay) in the case of quasistatic loading, i.e. when acceleration

* Corresponding author.
E-mail addresses: fredrik.larsson@chalmers.se (F. Larsson), kenneth.runesson@chalmers.se (K. Runesson).

http://dx.doi.org/10.1016/j.cma.2014.12.002

of both the solid skeleton and the pore fluid can be ignored. A wealth of literature has been devoted to the finite element solution of the coupled poroelasticity problem and its generalization to include materially nonlinear and rate-dependent effects; cf. Booker and coworkers [2–4], Runesson [5]. However, as it appears from the literature, very little attention has been paid to global error estimation and adaptive finite element techniques, in particular the appropriate space–time adaptive strategies. Limited attempts are those of Aubry et al. [6] and Hicks [7], who considered pure space-adaptivity, and those of Runesson et al. [8] and Larsson et al. [9], who considered pure time-adaptivity.

The general space–time adaptive procedure is far more challenging, cf., e.g., Eriksson et al. [10,11], Rannacher [12], Díez and Calderón [13], Ladevèze et al. [14] and Hoffman [15]. In particular when there is a strong transport phenomena, such as in structural dynamics, cf. Verdugo et al. [16], the optimal spatial mesh varies dramatically with time. Hence, there is a great need for arbitrary space–time adaptivity. Such a general scheme requires recursive adaptations of the whole space–time-mesh. In addition, existing error estimators for *global* error control in space–time require extensive data storage in terms of saving the complete time–history of the entire solution, cf. Chamoin and Ladevèze [17], Parés et al. [18,19] and Waeytens et al. [20]. Attempts of circumventing the need for such a complete recursive strategy normally involves global error control in space while restricting to local error control in time, cf. Aubry et al. [6].

In this paper, we present a strategy for obtaining global error control in quantities of interest via time-sequential space–time adaptivity, whereby the need for recursive computations and excessive data storage is avoided. In order to achieve this goal it is necessary to identify the error generation in space and time separately. This can be accomplished via a hierarchical decomposition of the discrete (finite element based) dual space. Indeed, this is a novel feature that is pursued in the present paper.

The paper is outlined as follows: To begin with, a quite broad class of time-dependent and nonlinear coupled problems is discussed in an abstract variational setting in space–time, whereby the framework is sufficiently general to allow for discontinuous discretization in time. Hence, the framework accommodates the dG(k)-methods. Next, the formally exact *a posteriori* error representation formula is presented for the space–time format, which is based on the solution of an appropriate dual problem. With such a formulation it is possible to choose any goal-oriented error measure in space–time, which is of engineering interest, cf. Prudhomme and Oden [21], Larsson et al. [22], Stein et al. [23]. The resulting error formula is manipulated (approximated) to allow for the identification of pure space error and pure time error, respectively. In particular, we discuss a sequential-adaptive strategy that involves adaptive change of the *current* space–time slab only in order to avoid full recursive adaptivity of the whole time–history.

Next, we apply the general strategy to the nonlinear consolidation problem in poromechanics. We then choose to control the error in displacement and pore pressure at a given spatial point after given time has elapsed or during a certain interval of time. The numerical results thoroughly demonstrate the good performance of the proposed sequential-adaptive algorithm. In particular, it is shown that the precision (in terms of effectivity index) can be quite acceptable for the considered problem; however, it is also noted that the optimal time-mesh is very sensitive to the particular choice of the goal function in space–time.

2. The abstract variational setting for a class of coupled problems

2.1. Continuous problem in space–time

2.1.1. Preliminaries

We shall establish the variational format in the space–time domain $S \stackrel{\text{def}}{=} \Omega \times I$, for given spatial domain Ω and time domain $I = (0, T)$, for a quite broad class of problems involving a first order time-derivative. In particular, the coupled problem of consolidation of geomaterials falls within this class. Another interesting application is the problem of dynamics, rewritten in first-order form, i.e. through a Hamiltonian description. It is of considerable interest to note from the outset that, due to the forward transport of information in time, it is always possible to consider a set of finite time intervals, whereby the solution at the end of any such interval will act as the initial data for the next one. To this end, we introduce a partition $0 = t_0 < t_1 < \cdots < t_N = T$ of the considered time domain $I = (0, T)$ into time-intervals $I_n = (t_{n-1}, t_n)$ of length $\Delta t_n = t_n - t_{n-1}$.[1] Hence, we define space–time slabs $S_n \stackrel{\text{def}}{=} \Omega \times I_n$ such that the space–time domain can be given as $S \stackrel{\text{def}}{=} \Omega \times I = S_1 \cup S_2 \cdots \cup S_n$.

[1] The abbreviated notation $\Delta t = \Delta t_n$ will be used henceforth for the current time step associated with I_n.

Next, we introduce the space $\mathbb{C}(S')$ defined on a space–time slab $S' \stackrel{\text{def}}{=} \Omega \times I'$ for a time-interval $I' \subseteq I$. The space $\mathbb{C}(S')$ is spanned by all functions for which (i) the weak form of the problem at hand is well-defined on S', and (ii) the Dirichlet-type boundary conditions on the (spatial) boundary of Ω are fulfilled. In conjunction with the solution space $\mathbb{C}$, we introduce the test-space $\mathbb{C}^0(S')$ that consists of functions that fulfill the same regularity requirements on S' as the functions in the solution space, but where the functions are homogeneous on the Dirichlet part of the boundary of Ω. We thus obtain the relation $z + \delta z \in \mathbb{C}(S')$ for any two functions $z \in \mathbb{C}(S')$ and $\delta z \in \mathbb{C}^0(S')$.

As a further preliminary, we also introduce the time-dependent spatial variational forms $a(z;\delta z)(t') = a(z|_{t=t'};\delta z|_{t=t'})$, $(z,\delta z)(t') = (z|_{t=t'},\delta z|_{t=t'})$ and $l(\delta z)(t') = l(\delta z|_{t=t'})$ on Ω for functions $z \in \mathbb{C}(S')$ and $\delta z \in \mathbb{C}^0(S')$ defined on $S' = \Omega \times I'$ with $I' \ni t'$.[2] The form $a(z;\delta z)$ is semi-linear (non-linear in z but linear in δz) and corresponds to the spatial weak form of the problem, $(z,\delta z)$ is the bi-linear scalar product in $L_2(\Omega)$, and $l(\delta z)$ is a linear functional that represents data to the problem. Such data are load/source in the interior of Ω and natural boundary conditions on the Neumann boundary part of Ω. Moreover, we introduce the (generally non-linear) differential operator $\Phi[z]$ in space that corresponds to a conservation quantity, i.e., the space–time PDE describes the evolution of $\Phi[z]$. We thus study a problem of which the spatial weak form, which is often utilized in conventional semi-discrete formulations, reads as follows:

$$(\mathrm{d}_t \Phi, \delta z) + a(z;\delta z) = l(\delta z) \quad t \in [0,T], \tag{1}$$

where d_t denotes the time derivative. The initial condition is given as $\Phi[z] = \Phi_0$ when $t = t_0 = 0$.

2.1.2. Weak format based on time-discontinuous solution and test spaces

Employing the time-dependent variational forms in space introduced above, we establish the full variational forms in space–time as follows:

$$A(z;\delta z) \stackrel{\text{def}}{=} \sum_{n=1}^{N} \int_{I_n} \left[(\mathrm{d}_t \Phi[z], \delta z) + a(z;\delta z)\right] \mathrm{d}t + \left(\Phi\left[z(t_0^+)\right], \delta z(t_0^+)\right) + \sum_{n=2}^{N} \left(\llbracket \Phi[z] \rrbracket(t_{n-1}), \delta z(t_{n-1}^+)\right) \tag{2}$$

$$L(\delta z) \stackrel{\text{def}}{=} \sum_{n=1}^{N} \int_{I_n} l(\delta z)\, \mathrm{d}t + \left(\Phi[z_0], \delta z(t_0^+)\right), \tag{3}$$

where z_0 represents the given initial value on z that is satisfied only in weak form in general, and where $\llbracket \Phi \rrbracket(t) \stackrel{\text{def}}{=} \Phi(t^+) - \Phi(t^-)$ denotes the jump of Φ at time t. From the construction of these forms, it is clear that we consider the situation when both z and δz may be time-discontinuous. Hence, we introduce the spaces of time-discontinuous functions

$$\mathbb{D} = \{z : z|_{S_n} \in {}^n\mathbb{D} \stackrel{\text{def}}{=} \mathbb{C}(S_n),\ n = 1,2,\ldots,N\}, \tag{4}$$

$$\mathbb{D}^0 = \{z : z|_{S_n} \in {}^n\mathbb{D}^0 \stackrel{\text{def}}{=} \mathbb{C}^0(S_n),\ n = 1,2,\ldots,N\}. \tag{5}$$

Here, we recall that $\mathbb{C}(S_n)$ denotes the space of functions on S_n that have sufficient regularity inside the slab, and that satisfy essential boundary conditions on the Dirichlet part of the boundary of Ω. The functions in $\mathbb{C}^0(S_n)$ possess the same regularity properties; however, they are homogeneous on the Dirichlet part of the boundary of Ω. From the construction of $\mathbb{D}$ and $\mathbb{D}^0$ in (4) and (5), respectively, we thus conclude that $z + \delta z \in \mathbb{D}$ for any two functions $z \in \mathbb{D}$ and $\delta z \in \mathbb{D}^0$.

We are now in the position to formulate the variational problem in space–time as follows: Find $z \in \mathbb{D}$ such that

$$A(z;\delta z) = L(\delta z) \quad \forall \delta z \in \mathbb{D}^0, \tag{6}$$

which is completely equivalent to Eq. (1) due to the choice of infinite-dimensional trial and test spaces in time.

For later use, we introduce the residual of any given $\bar{z} \in \mathbb{D}$ as

$$R(\bar{z};\delta z) = L(\delta z) - A(\bar{z};\delta z), \tag{7}$$

[2] In the following, we shall omit the time variable following the spatial forms while keeping in mind that $a(\bullet;\bullet)$, $(\bullet;\bullet)$ and $l(\bullet)$ are actually functions in time in the case the arguments are space–time functions.

and it follows from (6) that $R(z;\delta z)=0$. Moreover, we define the tangent form of A, denoted A', as the Gâteaux derivative

$$\begin{aligned} A'(z;\delta z,\delta z^*) &\stackrel{\text{def}}{=} \frac{\mathrm{d}}{\mathrm{d}\epsilon} A(z+\epsilon\delta z^*;\delta z)\big|_{\epsilon=0} \\ &= \sum_{n=1}^{N}\int_{I_n}\left[\left(\mathrm{d}_t\,\Phi'[z;\delta z^*],\delta z\right)+a'(z;\delta z,\delta z^*)\right]\mathrm{d}t \\ &\quad+\left(\Phi'[z(t_0^+);\delta z^*(t_0^+)],\delta z(t_0^+)\right)+\sum_{n=2}^{N}\left(\llbracket\Phi'[z;\delta z^*]\rrbracket(t_{n-1}),\delta z(t_{n-1}^+)\right). \end{aligned} \tag{8}$$

In (8), we introduced the derivatives

$$a'(z;\delta z,\delta z^*)\stackrel{\text{def}}{=}\frac{\mathrm{d}}{\mathrm{d}\epsilon}a(z+\epsilon\delta z^*;\delta z)\big|_{\epsilon=0}, \tag{9}$$

$$\Phi'[z;\delta z^*]\stackrel{\text{def}}{=}\frac{\mathrm{d}}{\mathrm{d}\epsilon}\Phi[z+\epsilon\delta z^*]\big|_{\epsilon=0}. \tag{10}$$

Now, because of the forward transport of information in time mentioned above, it is sufficient to consider the "incremental form" of (6) applied to the space–time slabs S_n in sequence as follows: Find $z|_{S_n}\in {}^n\mathbb{D}$ such that

$$A_1(z;\delta z)=L_1(\delta z)\quad\forall\delta z\in{}^1\mathbb{D}^0, \tag{11}$$

$$A_n(z;\delta z)=L_n(z(t_{n-1}^-);\delta z)\quad\forall\delta z\in{}^n\mathbb{D}^0,\ n>1 \tag{12}$$

where $z(t_{n-1}^-)$ is known from the previous increment. In ((11), (12)), we introduced the incremental forms

$$A_n(z;\delta z)\stackrel{\text{def}}{=}\int_{I_n}\left[\left(\mathrm{d}_t\,\Phi[z],\delta z\right)+a(z;\delta z)\right]\mathrm{d}t+\left(\Phi\left[z(t_{n-1}^+)\right],\delta z(t_{n-1}^+)\right), \tag{13}$$

$$L_1(\delta z)\stackrel{\text{def}}{=}\int_{I_1} l(\delta z)\,\mathrm{d}t+\left(\Phi_0,\delta z(t_0^+)\right), \tag{14}$$

$$L_n(z(t_{n-1}^-);\delta z)\stackrel{\text{def}}{=}\int_{I_n} l(\delta z)\,\mathrm{d}t+\left(\Phi\left[z(t_{n-1}^-)\right],\delta z(t_{n-1}^+)\right),\quad n>1. \tag{15}$$

Remark. Following the literature, e.g. Eriksson et al. [11], we may identify a fictitious "initial value" $z(t_0^-)$ from the identity

$$(\Phi[z(t_0^-)],\delta z(t_0^+))=(\Phi_0,\delta z(t_0^+)), \tag{16}$$

whereby ((12), (15)) hold also for $n=1$. Henceforth, we tacitly use this identity independent on whether $z(t_0^-)$ actually exists or not; hence, the relation (12) is valid also for $n=1$. □

We may construct the residual pertinent to each S_n as

$$R_n(\bar z;\delta z)=L_n(\bar z(t_{n-1}^-);\delta z)-A_n(\bar z;\delta z) \tag{17}$$

for any function $\bar z\in\mathbb{D}$. In view of ((11), (12)), the exact solution, z, satisfies

$$R_n(z;\delta z)=0\quad\forall\delta z\in{}^n\mathbb{D}^0 \tag{18}$$

for each increment $n=1,\dots,N$. Clearly, the solution that satisfies all the incremental problems ((11), (12)) also solves the global problem (6), since we have the important identity

$$\sum_{n=1}^{N}R_n(z;\delta z)=R(z;\delta z) \tag{19}$$

for any functions $z\in\mathbb{D}$ and $\delta z\in\mathbb{D}^0$.

For later use, we now define the tangent form of A_n, denoted A_n', as the Gâteaux derivative

$$A_n'(z;\delta z,\delta z^*) \stackrel{\text{def}}{=} \frac{\mathrm{d}}{\mathrm{d}\epsilon} A_n(z+\epsilon\delta z^*;\delta z)\big|_{\epsilon=0}$$
$$= \big(\Phi'[z(t_{n-1}^+);\delta z^*(t_{n-1}^+)],\delta z(t_{n-1}^+)\big) + \int_{I_n}\big[\big(\mathrm{d}_t\,\Phi'[z;\delta z^*],\delta z\big) + a'(z;\delta z,\delta z^*)\big]\,\mathrm{d}t \tag{20}$$

where we recall the spatial Gâteaux derivatives defined in (9) and (10).

Remark. Note that the introduction of time-discontinuities so far is not an approximation. Comparing with the more straightforward presentation, i.e. in Eriksson et al. [10], the sum of time-intervals in the global problem (6) should rather be viewed as a set of sequential (exact) variational problems of standard character. □

2.2. Space–time finite element formulation using discontinuous Galerkin in time

2.2.1. General case: dG(k)-method

We introduce finite element approximations in both space and time. For the time-discretization we shall adopt the class of dG(k)-methods, $k \geq 0$, with $k = 0$ as the basic choice. The temporal mesh-function is common for all spatial points and given by the partitioning $I = \bigcup_{n=1}^N I_n$ as defined in the previous subsection, whereas the spatial mesh $h_n(\boldsymbol{X}), \boldsymbol{X} \in \Omega$, is associated with the triangulation of Ω that is unique to each $I_n, n = 1,\ldots,N$. As a result, the space–time mesh is piecewise prismatic on each S_n.[3]

With these preliminaries we may now formulate the finite element problem. Since we adopt discontinuous Galerkin (dG), we utilize the weak format based on discontinuous solution and test spaces, cf. Section 2.1.2. In standard fashion, we thus seek the finite element solution $z_h \in \mathbb{D}_h \subset \mathbb{D}$ such that

$$A(z_h;\delta z_h) = L(\delta z_h) \quad \forall \delta z_h \in \mathbb{D}_h^0 \subset \mathbb{D}^0, \tag{21}$$

where we recall the weak form (6). Introducing the finite element spaces related to the triangulation $h_n(\boldsymbol{X})$ as ${}^n\mathbb{V}_h$ and ${}^n\mathbb{V}_h^0$ for the trial and test-spaces, respectively, we define the FE-spaces for a dG(k)-method in time as follows:

$${}^n\mathbb{D}_h = {}^n\mathbb{V}_h \times \mathcal{P}^k(I_n), \qquad {}^n\mathbb{D}_h^0 = {}^n\mathbb{V}_h^0 \times \mathcal{P}^k(I_n), \tag{22}$$

where $\mathcal{P}^k(I_n)$ denotes polynomials of order k in time on the interval I_n.

We note that the residual of the FE-solution $z_h \in \mathbb{D}_h$ is given from (7) as

$$R(z_h;\delta z) = L(\delta z) - A(z_h;\delta z) = A(z;\delta z) - A(z_h;\delta z) \tag{23}$$

for arbitrary $\delta z \in \mathbb{D}^0$, where (6) was used to give the last equality. Finally, the (non-linear) Galerkin orthogonality

$$R(z_h;\delta z_h) = 0 \quad \forall \delta z_h \in \mathbb{D}_h^0 \tag{24}$$

follows from (21).

In practice, we consider the "incremental form" (18) on space–time slabs S_n, in sequence for $n = 1,2,\ldots,N$, as follows: Find $z_h|_{S_n} \in {}^n\mathbb{V}_h \times \mathcal{P}^k(I_n)$ such that

$$A_n(z_h;\delta z_h) = L_n(z_h(t_{n-1}^-);\delta z_h) \quad \forall \delta z_h \in {}^n\mathbb{V}_h^0 \times \mathcal{P}^k(I_n), \tag{25}$$

where $z(t_{n-1}^-)$ is known from the previous increment. The incremental forms A_n and L_n were given in (13) and (15).

In general, (25) is non-linear and we have to adopt an iterative solution strategy. Here, we propose Newton iterations as the basic method, which requires the Gâteaux derivative of A_n, as defined in (20), and the residual of (25), as defined in (17),

$$R_n(\bar z;\delta z) \stackrel{\text{def}}{=} L_n(\bar z(t_{n-1}^-);\delta z) - A_n(\bar z;\delta z). \tag{26}$$

[3] This is a result of adopting a dG-method; the situation becomes slightly different when a cG-method is adopted.

For the time interval I_n, we thus iterate for $l = 1, 2, \ldots,$

$$z_h^{(l+1)}|_{S_n} = z_h^{(l)}|_{S_n} + \mathrm{d}z_h, \tag{27}$$

until (25) is satisfied within a given tolerance. In each Newton-step, we solve for the update $\mathrm{d}z_h \in \mathbb{V}_h^0 \times \mathcal{P}^k(I_n)$ such that

$$A_n'(z_h^{(l)}; \delta z_h, \mathrm{d}z_h) = R_n(z_h^{(l)}; \delta z_h) \quad \forall \delta z_h \in {}^n\mathbb{V}_h^0 \times \mathcal{P}^k(I_n). \tag{28}$$

2.2.2. Special case: dG(0)-method

In particular, we shall employ the simple dG(0)-method of piecewise constant functions in time, i.e. $z_h(\boldsymbol{X}, t) = {}^n z_h(\boldsymbol{X})$ for $t \in I_n$. In practice this means to solve for the spatial solutions ${}^n z_h \in {}^n\mathbb{V}_h$ for each time-step I_n.[4] The FE-problem, now purely spatial, thus reads: For $n = 1, \ldots, N$, find ${}^n z_h \in {}^n\mathbb{V}_h$ such that[5]

$$R_n({}^n z_h; \delta z_h) = \Delta t \left[\langle l(\delta z_h)\rangle_n - a({}^n z_h; \delta z_h)\right] - \left(\Phi[{}^n z_h] - \Phi[{}^{n-1} z_h], \delta z_h\right) = 0 \quad \forall \delta z_h \in {}^n\mathbb{V}_h^0 \tag{29}$$

or

$$(\Phi[{}^n z_h], \delta z_h) + \Delta t\, a({}^n z_h; \delta z_h) = (\Phi[{}^{n-1} z_h], \delta z_h) + \Delta t\, \langle l(\delta z_h)\rangle_n \quad \forall \delta z_h \in {}^n\mathbb{V}_h^0, \tag{30}$$

where $\langle l\rangle_n$ denotes the mean value of l on I_n, i.e.

$$\langle l\rangle_n \overset{\text{def}}{=} \frac{1}{\Delta t}\int_{I_n} l\, \mathrm{d}t, \tag{31}$$

and ${}^{n-1} z_h \in {}^{n-1}\mathbb{V}_h$ is known from the previous time-step.[6]

The Gâteaux-derivative A_n', used in the Newton-iterations, becomes

$$A_n'(z_h; \delta z_h, \delta z_h^*) = \left(\Phi'[{}^n z_h; \delta z_h^*], \delta z_h\right) + \Delta t\, a'({}^n z_h; \delta z_h, \delta z_h^*). \tag{32}$$

The Newton-step, given by (28), can thus be rephrased more explicitly as

$$\left(\Phi'[{}^n z_h^{(l)}; \mathrm{d}z_h], \delta z_h\right) + \Delta t\, a'({}^n z_h^{(l)}; \delta z_h, \mathrm{d}z_h) = R_n(z_h^{(l)}; \delta z_n) \quad \forall \delta z_h \in {}^n\mathbb{V}_h^0. \tag{33}$$

2.3. Computation of space–time error based on the dual solution

We wish to control the error of the FE-solution $z_h \in \mathbb{D}_h$ in terms of a scalar goal function $Q(z)$ of engineering interest, and we define the error as

$$E(z, z_h) \overset{\text{def}}{=} Q(z) - Q(z_h). \tag{34}$$

It is noted that $Q(z)$ does not need to be a norm, nor does it need to be a linear functional of z.

With $\bar{z}(s) \overset{\text{def}}{=} z_h + s(z - z_h)$, $e = z - z_h$, we define the secant forms A_{S} and Q_{S} as follows:

$$\begin{aligned} A(z; \delta z) - A(z_h; \delta z) &= \int_0^1 \frac{\mathrm{d}}{\mathrm{d}s} A(\bar{z}(s); \delta z)\mathrm{d}s = \int_0^1 A'(\bar{z}(s); \delta z, e)\mathrm{d}s \\ &\overset{\text{def}}{=} A_{\mathrm{S}}(z, z_h; \delta z, e), \end{aligned} \tag{35}$$

[4] The only way that ${}^n\mathbb{V}_h$ differs for different values of n is that the Dirichlet boundary conditions may change with time. In fact, even the extension of the Dirichlet part of the boundary may be time-dependent.

[5] For brevity the notation δz_h is used for functions in ${}^n\mathbb{V}_h^0 \times \mathcal{P}^k(I_n)$ as well as for functions in ${}^n\mathbb{V}_h^0$. This is the case in (29).

[6] In analogy with the Remark above, we make the tacit interpretation $\left(\Phi[{}^0 z_h], \delta z_h\right) = (\Phi_0, \delta z_h) \quad \forall \delta z_h \in {}^1\mathbb{V}_h^0$, whereby (29) is valid also for $n = 1$.

$$Q(z) - Q(z_h) = \int_0^1 \frac{\mathrm{d}}{\mathrm{d}s} Q(\bar{z}(s))\mathrm{d}s = \int_0^1 Q'(\bar{z}(s); e)\mathrm{d}s \stackrel{\text{def}}{=} Q_{\mathrm{S}}(z, z_h; e). \tag{36}$$

In (36), we introduced the tangent form $Q'(z; \delta z^*)$ as the Gâteaux-derivative of Q in complete analogy with A' in (8).

Next, we introduce the appropriate dual solution $z^* \in \mathbb{D}^0$, which solves the (generally nonlinear) dual problem

$$A_{\mathrm{S}}(\bullet; z^*, \delta z^*) = Q_{\mathrm{S}}(\bullet; \delta z^*), \quad \forall \delta z^* \in \mathbb{D}^0. \tag{37}$$

We then obtain, by definition, the error representation

$$E(\bullet) \stackrel{(36)}{=} Q_{\mathrm{S}}(\bullet; e) \stackrel{(37)}{=} A_{\mathrm{S}}(\bullet; z^*, e) \stackrel{(35),(23)}{=} R(z_h; z^*). \tag{38}$$

In practice, it is necessary to introduce approximations (from linearization) at the computation of A_{S} and Q_{S} in (37), which introduces a linearization error. The most straightforward approximation is to replace the secant with the tangent at the known solution z_h, i.e.

$$A_{\mathrm{S}}(z, z_h; z^*, \delta z^*) \approx A_{\mathrm{S}}(z_h, z_h; z^*, \delta z^*) = A'(z_h; z^*, \delta z^*), \tag{39}$$

$$Q_{\mathrm{S}}(z, z_h; \delta z^*) \approx Q_{\mathrm{S}}(z_h, z_h; \delta z^*) = Q'(z_h; \delta z^*). \tag{40}$$

Henceforth, this approximation is used if nothing else is stated. Moreover, it is necessary to compute z^* by suitable space–time discretization; see further below.

As to the explicit structure of the dual problem (37), it is illuminating to elaborate on the expression for A' in (8). Upon integrating by parts in time on each I_n and then rearranging terms, we obtain

$$\begin{aligned} A'(z; \delta z, \delta z^*) &= \sum_{n=1}^{N} \Big\{ \int_{I_n} \left[-\left(\Phi'[z; \delta z^*], \mathrm{d}_t \delta z \right) + a'(z; \delta z, \delta z^*) \right] \mathrm{d}t \\ &\quad - (\Phi'[z(t_n^-); \delta z^*(t_n^-)], [\![\delta z]\!](t_n)) \Big\} + (\Phi'[z(t_N^-); \delta z^*(t_N^-)], \delta z(t_N^+)) \\ &\stackrel{\text{def}}{=} A^*(z; \delta z^*, \delta z). \end{aligned} \tag{41}$$

Upon introducing the form associated with each I_n

$$A_n^*(z; \delta z^*, \delta z) = \int_{I_n} \left[-(\Phi'[z; \delta z^*], \mathrm{d}_t \delta z) + a'(z; \delta z, \delta z^*) \right] \mathrm{d}t + (\Phi'[z(t_n^-); \delta z^*(t_n^-)], \delta z(t_n^-)) \tag{42}$$

we may express A^* as

$$A^*(z; \delta z^*, \delta z) = \sum_{n=1}^{N} \left[A_n^*(z; \delta z^*, \delta z) - (\Phi'[z(t_n^-); \delta z^*(t_n^-)], \delta z(t_n^+)) \right] + (\Phi'[z(t_N^-); \delta z^*(t_N^-)], \delta z(t_N^+)). \tag{43}$$

Moreover, we decompose the goal-functional Q into

$$Q(z) = \sum_{n=1}^{N} Q_n(z) + \bar{Q}(z(T)), \tag{44}$$

where Q_n are space–time functionals on the open time-intervals I_n, and $\bar{Q}$ is a space-functional to be evaluated at $t = T$. Hence, we obtain the forms associated with the dual loading as follows:

$$L_N^*(z; \delta z^*) = \bar{Q}'(z(t_N^-); \delta z^*(t_N^-)) + Q_N'(z; \delta z^*) \tag{45}$$

$$L_n^*(z; \delta z^*, z^*(t_n^+)) = (\Phi'[z(t_n^-); \delta z^*(t_n^-)], z^*(t_n^+)) + Q_n'(z; \delta z^*), \quad n < N. \tag{46}$$

It is noted that (37) represents a time-dependent problem running backwards in time from $t = t_N$. Hence, we may consider the "incremental form" of (37) applied to the space–time slabs S_n in sequence for $n = N, N-1, \ldots, 1$ as

follows: Find $z^*|_{S_n} \in \mathbb{C}^0(S_n)$ such that

$$A_N^*(z_h; \delta z^*, z^*) = L_N^*(z_h; \delta z^*), \quad \forall \delta z^* \in \mathbb{C}^0(S_N), \tag{47}$$

$$A_n^*(z_h; \delta z^*, z^*) = L_n^*(z_h; \delta z^*, z^*(t_n^+)), \quad \forall \delta z^* \in \mathbb{C}^0(S_n),\ n < N, \tag{48}$$

where $z^*(t_n^+)$ is known from the previous increment.

Remark. Like in the case of the initial value for the primal problem, we may identify a fictitious "initial value" $z^*(t_N^+)$ from the identity

$$(\Phi'[z(t_N^-); \delta z^*(t_N^-)], z^*(t_N^+)) = \bar{Q}'(z(t_N^-); \delta z^*(t_N^-)), \quad \forall \delta z^* \in \mathbb{C}^0(S_N) \tag{49}$$

whereby (46) holds also for $n = N$. Henceforth, we tacitly use this identity independent on whether $z^*(t_N^+)$ actually exists or not; hence, the relation (48) is valid also for $n = N$.

Let us consider a few important examples of goal functionals $\bar{Q}$ where it is possible to directly identify $z^*(t_N^-)$:

1. $\bar{Q}(z(T)) = (\Phi[z(T)], \psi)$, where $\psi = \psi(\boldsymbol{X})$ is an *extraction function* on Ω_0, then

$$\bar{Q}'(z(t_N^-); \delta z^*(t_N^-)) = (\Phi'[z(t_N^-); \delta z^*(t_N^-)], \psi), \quad \forall \delta z^* \in \mathbb{C}^0(S_N) \tag{50}$$

   and from (49) we conclude that the "initial condition" is $z^*(t_N^+) = \psi$.
2. $\bar{Q}(z(T)) = \|\Phi[z(T)]\|$, where $\|\bullet\|$ represents the L_2 norm on Ω_0, then

$$\bar{Q}'(z(t_N^-); \delta z^*(t_N^-)) = \frac{1}{\|\Phi[z(t_N^-)]\|}(\Phi'[z(t_N^-); \delta z^*(t_N^-)], \Phi[z(t_N^-)]), \quad \forall \delta z^* \in \mathbb{C}^0(S_N) \tag{51}$$

   and from (49) we conclude that the "initial condition" is $z^*(t_N^+) = \Phi[z(t_N^-)]/\|\Phi[z(t_N^-)]\|$, which depends on the primal solution z. □

Finally in this subsection, we give the more explicit expression for the error representation, given generally in (38), in the particular case that the dG(0)-method has been used for computing the FE-solution z_h. In this case we obtain from (26)

$$R(z_h; z^*) = \sum_{n=1}^{N} R_n(z_h; z^*), \tag{52}$$

with

$$R_n(z_h; z^*) = \Delta t \left[\langle l(z^*)\rangle_n - a({}^n z_h; \langle z^*\rangle_n)\right] - (\Phi[{}^n z_h] - \Phi[{}^{n-1} z_h], z^*(t_{n-1}^+)). \tag{53}$$

2.4. Space–time finite element format of the dual problem

2.4.1. General case: dG(k)-method

When a dG(k)-method is used for the time-integration of the dual problem (48) on incremental form, the FE-problem becomes: Find $z_h^*|_{S_n} \in {}^n\mathbb{V}_h^0 \times \mathcal{P}^k(I_n)$ such that, in sequence for $n = N, N-1, \ldots, 1$,

$$A_n^*(z_h; \delta z_h^*, z_h^*) = L_n^*(z_h; \delta z_h^*, z_h^*(t_n^+)), \quad \forall \delta z_h^* \in {}^n\mathbb{V}_h^0 \times \mathcal{P}^k(I_n). \tag{54}$$

It is noted that this problem is linear in z_h^* (due to the introduced linearizations).

2.4.2. Special case: dG(0)-method

In the particular case that dG(0) is employed, we may rephrase (54) as a purely spatial problem for each time step I_n (as for the primal problem): For $n = N, N-1, \ldots, 1$, find ${}^n z_h^* \in {}^n\mathbb{V}_h^0$ such that

$$(\Phi'[{}^n z_h, \delta z_h^*], {}^n z_h^*) + \Delta t\, a'({}^n z_h; {}^n z_h^*, \delta z_h^*) = (\Phi'[{}^n z_h, \delta z_h^*], {}^{n+1} z_h^*), \quad \forall \delta z_h^* \in {}^n\mathbb{V}_h^0 \tag{55}$$

where ${}^{n+1} z_h^*$ is known from the previous time-step.[7]

[7] We make the tacit interpretation $\left(\Phi'[{}^N z_h, \delta z_h^*], {}^{N+1} z_h^*\right) = Q_T'\left({}^N z_h, \delta z_h^*\right) \quad \forall \delta z_h^* \in {}^N\mathbb{V}_h^0$, whereby (55) is valid also for $n = N$.

3. Computational strategy

3.1. Preliminaries

In this section, the novel strategy for sequential adaptive computations will be presented. A few important computational issues will be discussed subsequently. They can be categorized as:

- Computation of an approximate dual solution z^*. The main strategy is to introduce a *hierarchical* decomposition of the dual solution space, leading to additive decomposition of the dual solution into parts that represent space and time error, respectively. *Note*: An additive decomposition of the dual solution gives an additive decomposition of the computed error.
- Efficient strategy for adaptation of the space–time mesh on space–time slabs S_n without the need for recursive adaptations of the whole time-mesh. The goal is to fully adaptively define the space-mesh and the time-step of each S_n in a truly sequential fashion for $i = 1, 2, \ldots, N$, whereby it is noted that the number of time intervals, N, is a result of the adaptive procedure.

Remark. It is straightforward to incorporate the solution error, in addition to the usual FE-discretization error. The FE-error is the difference between the exact solution z and the exact solution of the variationally consistent problem obtained from discretization, denoted z_h. The solution error is, in principle, the difference between z_h and the actual computational result, denoted z_h^{SOL} henceforth. This error may have different sources (known or unknown). An example of such sources is incomplete iterations in a Newton iteration algorithm. □

In order to be specific, although with minor loss of generality, we shall henceforth consider 2D-problems only. Moreover, we shall assume that the FE-space ${}^n\mathbb{V}_h$ contains standard piecewise linear approximation on triangular spatial meshes (as the simplest possible choice),[8] while the dG(0)-method is used in time.'

3.2. Computation of the dual solution in space–time

3.2.1. Approximations in the dual problem

As to the practical computation of the dual solution $z^* \in \mathbb{D}^0$, we note that two principally different sources of error arise: (1) The dual problem (37) is linearized such that the secant forms $A_{\mathrm{S}}(z, z_h; z^*, \delta z^*)$ and $Q_{\mathrm{S}}(z, z_h; \delta z^*)$, which depend on the exact (unknown) solution z, are replaced by the tangent forms $A'(z_h; z^*, \delta z^*)$ and $Q'(z_h; \delta z^*)$ evaluated at the FE-solution z_h. (2) The exact solution $z^* \in \mathbb{D}^0$ is approximated with some suitable $\tilde{z}^* \in \tilde{\mathbb{D}}^0$, which is considered as an *enhancement* of the ordinary FE-solution $z_h^* \in \mathbb{D}_h^0$. Clearly, z_h^* is completely ineffective as a direct approximation of z^*, since it will not give any contribution to the error in view of the Galerkin orthogonality.

3.2.2. Decomposition of the enhanced functions spaces

We now consider an approximation $\tilde{z}^* \in \tilde{\mathbb{D}}^0$. In order to decompose the error estimate into spatial and temporal parts, we will consider the influence of the dual approximation on the residual.

One possible strategy is to introduce a *hierarchical enhancement* upon introducing the decomposition

$$\tilde{\mathbb{D}}^0 = \{z|_{S_n} \in {}^n\tilde{\mathbb{D}}^0\} \quad \text{with } {}^n\tilde{\mathbb{D}}^0 = {}^n\tilde{\mathbb{V}}_h^0 \times \tilde{\mathcal{P}}^0(I_n) = \mathbb{D}_h^0 \oplus \Delta\overset{(\mathrm{s})}{\mathbb{D}}{}_h^0 \oplus \Delta\overset{(\mathrm{t})}{\mathbb{D}}{}_h^0 \oplus \Delta\overset{(\mathrm{st})}{\mathbb{D}}{}_h^0 \tag{56}$$

such that $\tilde{z}^*$ can be decomposed additively as

$$\tilde{z}^* = \tilde{z}_h^* + \Delta\overset{(\mathrm{s})}{z}{}_h^* + \Delta\overset{(\mathrm{t})}{z}{}_h^* + \Delta\overset{(\mathrm{st})}{z}{}_h^* \tag{57}$$

with $\tilde{z}_h^* \in \mathbb{D}_h^0$, $\Delta\overset{(\mathrm{s})}{z}{}_h^* \in \Delta\overset{(\mathrm{s})}{\mathbb{D}}{}_h^0$, $\Delta\overset{(\mathrm{t})}{z}{}_h^* \in \Delta\overset{(\mathrm{t})}{\mathbb{D}}{}_h^0$ and $\Delta\overset{(\mathrm{st})}{z}{}_h^* \in \Delta\overset{(\mathrm{st})}{\mathbb{D}}{}_h^0$. Hence, we have decomposed $\tilde{z}^*$ into contributions from the regular FE-space $\mathbb{D}_h^0$, a purely spatial enhancement $\Delta\overset{(\mathrm{s})}{z}{}_h^*$, a purely temporal enhancement $\Delta\overset{(\mathrm{t})}{z}{}_h^*$ and a mixed spatial/temporal enhancement $\Delta\overset{(\mathrm{st})}{z}{}_h^*$.

[8] Here, we assume the approximation to be numerically stable, i.e., we assume that the Babushka–Brezzi inf-sup condition is satisfied if relevant.

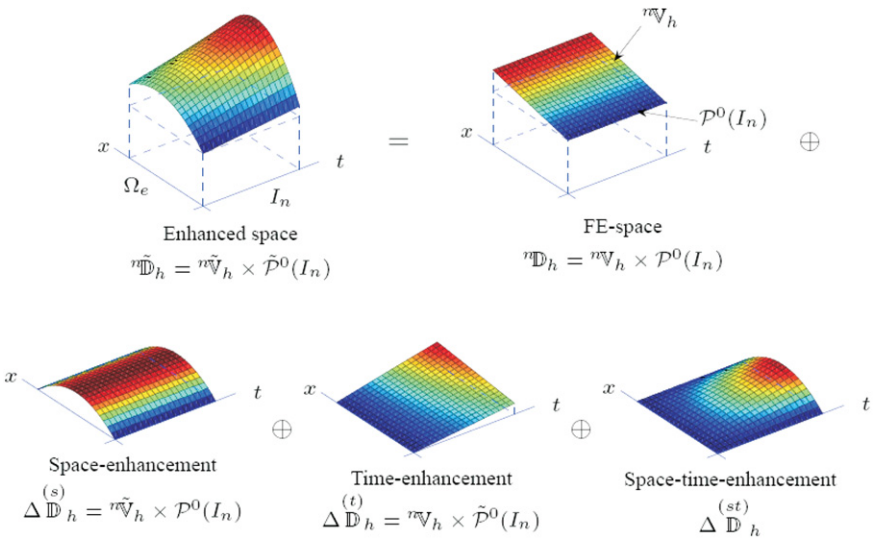

Fig. 1. Illustration of hierarchical decomposition of the enhanced dual solution on a space–time element (1D-space).

Remark. The linear part $\tilde{z}_h^* \in \mathbb{D}_h^0$ is *not* identical to the regular FE-solution $z_h^* \in \mathbb{D}_h^0$, although both $\tilde{z}_h^*$ and z_h^* belong to the same space $\mathbb{D}_h^0$ (piecewise linear in space and $\mathcal{P}^0(I_n)$ in time). However, they both qualify in the Galerkin orthogonality. □

We may now obtain the approximate error representation as

$$\underbrace{R(z_h;\tilde{z}^*)}_{\simeq E_{\mathrm{FEM}}} = \underbrace{R(z_h;\Delta\overset{(s)}{z}{}_h^* + \frac{1}{2}\Delta\overset{(st)}{z}{}_h^*)}_{\equiv \overset{(s)}{E}_{\mathrm{FEM}}} + \underbrace{R(z_h;\Delta\overset{(t)}{z}{}_h^* + \frac{1}{2}\Delta\overset{(st)}{z}{}_h^*)}_{\equiv \overset{(t)}{E}_{\mathrm{FEM}}} \tag{58}$$

where we used the Galerkin orthogonality to drop the contribution from $\tilde{z}_h^*$, since $R(z_h;\tilde{z}_h^*) = 0$.

Remark. Note that we here tacitly choose to split the (higher order) mixed term and divide it between the spatial and temporal error contributions. □

As to the enhancement in space, we simply choose ${}^n\tilde{\mathbb{V}}_h$ as piecewise quadratics on each triangular element. The straightforward enhancement in time would be to set $\tilde{\mathcal{P}}^0(I_n) = \mathcal{P}^1(I_n)$, corresponding to dG(1). However, in order to reduce the computational effort, we rather opt for a suitable smoothing procedure based on the dG(0)-solution and leading to piecewise linear variation in each I_n, while capturing possible discontinuities at each time node t_n. The space–time decomposition is shown schematically in Fig. 1 for a single space–time element.

3.2.3. Slab-wise computation of the enhanced dual solution

We shall now describe a procedure for computing the components of the dual solution, given in (57), on each space–time slab S_n.

Firstly, we compute the enhanced solution in space by solving on the enhanced spatial discretization for dG(0) in time. Based on an end condition at time t_n^+, we thus compute $\tilde{z}^{*,-} \in \tilde{\mathbb{V}}_h^0$ such that

$$(\Phi'[{}^n z_h, \delta z^*], \tilde{z}^{*,-}) + \Delta t\, a'({}^n z_h; \tilde{z}^{*,-}, \delta z^*) = (\Phi'[{}^n z_h, \delta z^*], \tilde{z}^*(t_n^+)), \quad \forall \delta z^* \in \tilde{\mathbb{V}}_h^0 \tag{59}$$

where $\tilde{\mathbb{V}}_h^0$ is the space described by higher order elements (piecewise quadratics) than $\mathbb{V}_h^0$. Eq. (59) is thus the spatially enhanced version of Eq. (55).

Using nodal interpolation onto the linear shape functions, defined by Π_h, we compute the contributions as

$$\tilde{z}_h^* = \Pi_h \tilde{z}^{*,-}, \qquad \Delta\overset{(s)}{z}{}_h^* = (1 - \Pi_h)\,\tilde{z}^{*,-}. \tag{60}$$

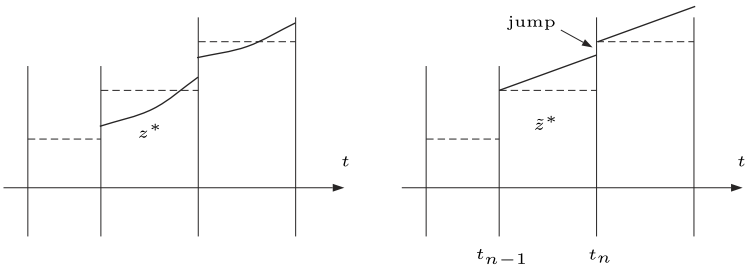

Fig. 2. Method for computing time-enhancement of the dual solution. Left figure shows the exact, possibly discontinuous, solution and the dG(0) solution. Right figure shows the Discontinuous Smoothed dG(0) solution.

Secondly, we follow along the lines of Larsson et al. [24] and compute the *Discontinuous Smoothed dG(0)* approximation as follows: A short backwards time-step approximation $\tilde{z}^{*,+} \in \tilde{\mathbb{V}}_h^0$ is computed from

$$(\Phi'[{}^n z_h, \delta z^*], \tilde{z}^{*,+}) + (1-\beta)\Delta t\, a'({}^n z_h; \tilde{z}^{*,+}, \delta z^*) = (\Phi'[{}^n z_h, \delta z^*], \tilde{z}^*(t_n^+)), \quad \forall \delta z^* \in \tilde{\mathbb{V}}_h^0 \tag{61}$$

where, typically, we choose $\beta = 0.99$. This step is to capture the discontinuity of the exact dual solution, cf. Fig. 2.

Using linear interpolation in time, we finally identify the components

$$\Delta \overset{(t)}{z}{}^* = \frac{t-t_{n-1}}{\beta\Delta t}\Pi_h\left[\tilde{z}^{*,+} - \tilde{z}^{*,-}\right], \qquad \Delta \overset{(st)}{z}{}^* = \frac{t-t_{n-1}}{\beta\Delta t}(1-\Pi_h)\left[\tilde{z}^{*,+} - \tilde{z}^{*,-}\right]. \tag{62}$$

3.2.4. Solution error in the space–time FE-solution

It is straightforward to account for the solution error that arises due to the fact that the computed solution $z_h^{\mathrm{SOL}} \neq z_h$ in practice. It is then realized that, since z_h is never computed, it is necessary to replace the (approximate) dual problem (48) with the (even more approximate) problem

$$A_n^*(z_h^{\mathrm{SOL}}; \delta z^*, z^*) = L_n^*(z_h^{\mathrm{SOL}}; \delta z^*, z^*(t_n^+)), \quad \forall \delta z^* \in {}^n\mathbb{D}^0, \tag{63}$$

where, for the sake of simplicity, z^* denotes the exact solution to the *approximate* dual problem (63). Note that, although $z_h^{\mathrm{SOL}} \in \mathbb{D}_h^0$, it does not necessarily satisfy the Galerkin orthogonality, i.e. in general we have

$$R(z_h^{\mathrm{SOL}}; \delta z_h) \neq 0 \tag{64}$$

for any given $\delta z_h \in {}^n\mathbb{D}^0$. While it is still possible to make the hierarchical decomposition of $\tilde{z}^*$, described above, the error representation now becomes

$$E(z, z_h^{\mathrm{SOL}}) \simeq R(z_h^{\mathrm{SOL}}; \tilde{z}^*), \tag{65}$$

with

$$\underbrace{R(z_h^{\mathrm{SOL}}; \tilde{z}^*)}_{\simeq E} = \underbrace{R(z_h^{\mathrm{SOL}}; \tilde{z}_h^*)}_{\simeq E_{\mathrm{SOL}}} + \underbrace{R(z_h^{\mathrm{SOL}}; \Delta \overset{(s)}{z}{}_h^* + \frac{1}{2}\Delta \overset{(st)}{z}{}_h^*)}_{\equiv \overset{(s)}{E}_{\mathrm{FEM}}} + \underbrace{R(z_h^{\mathrm{SOL}}; \Delta \overset{(t)}{z}{}_h^* + \frac{1}{2}\Delta \overset{(st)}{z}{}_h^*)}_{\equiv \overset{(t)}{E}_{\mathrm{FEM}}}. \tag{66}$$

Remark. As discussed above, it is possible to compute the hierarchical contributions approximately upon assuming that $\tilde{z}_h^* \simeq z_h^*$. In such a case, we have

$$E_{\mathrm{SOL}} \simeq R(z_h^{\mathrm{SOL}}; z_h^*), \tag{67}$$

whereas the different contributions to E_{FEM} are still given formally as in (66). □

A strategy for controlling independently $\overset{(s)}{E}_{\mathrm{FEM}}$ and $\overset{(t)}{E}_{\mathrm{FEM}}$, as part of an adaptive procedure, is outlined in the next subsection.

3.3. Sequential-adaptive strategy for the space–time slabs

Our aim is to device an adaptive strategy in space–time that is computationally efficient. It is then highly desirable to avoid concurrent space–time remeshing of $S = \Omega \times I$. We rather opt for an algorithm that allows for *sequential* adaptive space–time remeshing of each $S_n = \Omega \times I_n$, whereby the space-mesh $\mathcal{M}_{h,n}^{\text{space}}$ and I_n are determined concurrently. In other words, each S_n is adaptively remeshed only *once*. Although this seems like a modest requirement, it is not trivial due to the fact that error transport from S_n depends on all other space–time slabs $S_{n+1}, S_{n+2}, \ldots$ up to the last point in time for which we wish to control the error.

As the first ingredient in the proposed strategy, we *allow for*[9] the rate of error accumulation (including generation and transport) to be *uniform* in time, i.e. the stopping criterion is given, for any considered S_n, as follows:

$$E_n \overset{\text{def}}{=} E_{n,\text{SOL}} + E_{n,\text{FEM}} \leq \text{TOL}\frac{\Delta t_n}{T} \tag{68}$$

subjected to the constraint condition

$$\alpha^- \overset{(t)}{E}_{n,\text{FEM}} \leq \overset{(s)}{E}_{n,\text{FEM}} \leq \alpha^+ \overset{(t)}{E}_{n,\text{FEM}} \tag{69}$$

where $\alpha^+ \geq \alpha^- > 0$ are "sufficiently close". Clearly, $\alpha^- = \alpha^+ = 0.5$ would correspond to equilibrated space–time error on each S_n.

The second (and key) ingredient in the adaptive algorithm is that the dual solution computed on the *initial space–time mesh* plays a key role throughout the adaptive procedure, which is outlined as follows:

1. For given initial (say uniform) space–time mesh $\mathcal{M}_H \overset{\text{def}}{=} \mathcal{M}_h^{(0)}$, compute the FE-solution z_H.
2. Based on z_H, compute the background dual FE-solution z_H^* on $\mathcal{M}_H$ using the basic FE-method, and carry out *continuous* smoothing in time to obtain the time-enhanced solution $\tilde{z}_H^*$. This dual solution is now stored.
3. For $n = 1, 2, \ldots$, establish the space-mesh $\mathcal{M}_{h,n}^{\text{space}}$ and the current time interval I_n adaptively. This is done, for each adaptive iteration (k) according to the Box I, cf. also Fig. 3. After convergence of the adaptive procedure, then the set $\{\mathcal{M}_{h,n}\}_{n=1}^N$ and the set $\{I_n\}_{n=1}^N$ have been determined.

Remark. It should be noted that, due to the dG-formulation in time, initial conditions for the primal solution, as well as end-conditions for the dual solution, are naturally given by the L_2-projection if the spatial mesh varies from one slab to another. □

4. Consolidation of binary porous medium

4.1. Strong format in space–time

We consider the problem of consolidation of a poroelastic body (soil), whose mechanical state is determined by the displacement field $\boldsymbol{u}(\boldsymbol{X}, t)$ and intrinsic pore pressure field $p(\boldsymbol{X}, t)$ for $\boldsymbol{X} \in \Omega_0$ and $t \in I$. Finite deformations are considered such that Ω_0 represents the initial configuration at $t = t_0 = 0$. The boundary Γ_0 of Ω_0 is divided into Dirichlet and Neumann parts in two different ways; $\Gamma_0 = \Gamma_{0,\text{D}}^{(1)} \cup \Gamma_{0,\text{N}}^{(1)} = \Gamma_{0,\text{D}}^{(2)} \cup \Gamma_{0,\text{N}}^{(2)}$. Firstly, the displacements are prescribed on $\Gamma_{0,\text{D}}^{(1)}$, whereas surface tractions are prescribed on $\Gamma_{0,\text{N}}^{(1)}$. Secondly, the (excess) pore pressure is prescribed on $\Gamma_{0,\text{D}}^{(2)}$, whereas the drainage velocity is prescribed on $\Gamma_{0,\text{N}}^{(2)}$. It is assumed that no volume loads act in the interior of Ω_0 (for simplicity).

The strong form of the consolidation problem can now be formulated in terms of the two balance equations[10]:

$$-\boldsymbol{P} \cdot \overleftarrow{\nabla}_X = \boldsymbol{0} \quad \text{in } \Omega_0 \times I, \tag{70}$$

[9] Note that this is merely a choice for distributing the error, and thus designing the discretization in space and time.

[10] Henceforth, we introduce the notation $\overleftarrow{\nabla}$ for the differential operator acting in the left direction, e.g. $\boldsymbol{P} \cdot \overleftarrow{\nabla} = \sum_{j=1}^3 \frac{\partial P_{ij}}{\partial X_j} \boldsymbol{E}_i$ in Cartesian coordinates with basis $\{\boldsymbol{E}_j\}_{i=1}^3$.

1. Compute $z_h|_{S_n^{(k)}}$ based on $z_h(t_{n-1}^-)$ that was computed for the previous time slab S_{n-1}. Then, solve for the enhanced dual solution $\tilde{z}^*|_{S_n^{(k)}}$ from the *decoupled* dual problem

   $$A_n^*(z_h^{(k)};\delta z^*,\tilde{z}^{*(k)}) = L_n^*(z_h^{(k)};\delta z^*,\tilde{z}_H^*(t_n^+)),$$

   whereby it is noted that $\tilde{z}^*(t_n^+)$ has been replaced by the background dual solution $\tilde{z}_H^*(t_n^+)$ as the load (or data) for the current space–time slab.
2. Compute the error contributions $E_{n,\mathrm{SOL}}^{(k)}$, $\overset{(s)}{E}{}_{n,\mathrm{FEM}}^{(k)}$, etc.
3. Check the stopping criterion in (68): If

   $$E_n^{(k)} \le \mathrm{TOL}\frac{\Delta t_n^{(k)}}{T}$$

   then exit and take a new time step.
4. Refine the space-mesh, the time interval or both: If

   $$\alpha^- \overset{(t)}{E}{}_{n,\mathrm{FEM}}^{(k)} \le \overset{(s)}{E}{}_{n,\mathrm{FEM}}^{(k)} \le \alpha^+ \overset{(t)}{E}{}_{n,\mathrm{FEM}}^{(k)}$$

   then refine in space and time uniformly.
   Else if

   $$\alpha^+ \overset{(t)}{E}{}_{n,\mathrm{FEM}}^{(k)} \le \overset{(s)}{E}{}_{n,\mathrm{FEM}}^{(k)}$$

   then refine in space: $\mathcal{M}_{h,n}^{(k)} \to \mathcal{M}_{h,n}^{(k+1)}$, $I_n^{(k)} = I_n^{(k+1)}$
   Else if

   $$\overset{(s)}{E}{}_{n,\mathrm{FEM}}^{(k)} \le \alpha^- \overset{(t)}{E}{}_{n,\mathrm{FEM}}^{(k)}$$

   then refine in time: $I_n^{(k)} \to I_n^{(k+1)}$, $\mathcal{M}_{h,n}^{(k)} = \mathcal{M}_{h,n}^{(k+1)}$

Box I. Sequential-adaptive strategy for space–time slab S_n.

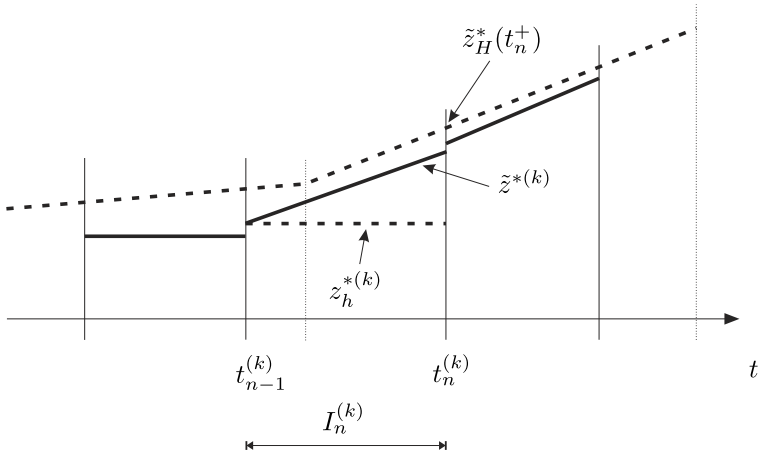

Fig. 3. Step k in the adaptation of $S_n^{(k)}$; enhanced solution $\tilde{z}^{*(k)}$ computed based on the FE-solution $z_h^{*(k)}$ (from Discontinuous Smoothed dG(0)-method) and data $\tilde{z}_H^*(t_n^+)$.

$$\mathrm{d}_t\left(Jn\rho^{\mathrm{f}}\right) + \nabla_X\cdot\left(\rho^{\mathrm{f}}\boldsymbol{W}\right) = 0 \quad \text{in } \Omega_0\times I, \tag{71}$$

whereby (70) represents the total quasistatic equilibrium (without acceleration) of the porous body, whereas (71) represents mass-conservation of the fluid occupying the pores of the porous body.

In (70) we introduced the total 1st Piola–Kirchhoff stress, $\boldsymbol{P}$, which can be split additionally into the solid (or effective) stress, $\boldsymbol{P}^{\mathrm{s}}$, and the fluid stress, $\boldsymbol{P}^{\mathrm{f}}$, measured per unit volume of the bulk (mixture). Moreover, the fluid stress is expressed in terms of the *intrinsic* pressure in the fluid, $\boldsymbol{P}^{\mathrm{f}} = -pJn\boldsymbol{F}^{-\mathrm{T}}$, where $J = \det(\boldsymbol{F})$ with $\boldsymbol{F} \overset{\text{def}}{=} \boldsymbol{I} + \boldsymbol{u} \otimes \overleftarrow{\nabla}_X = \boldsymbol{I} + \boldsymbol{H}$ with the displacement gradient defined as $\boldsymbol{H} \overset{\text{def}}{=} \boldsymbol{u} \otimes \overleftarrow{\nabla}_X$, and where n is the porosity.[11] In (71), we introduced (in addition) the intrinsic density of the fluid, ρ^{f}, and the Piola–Darcy-seepage velocity $\boldsymbol{W}$.

Assuming *intrinsic* incompressibility of the solid particles, i.e. $\rho^{\mathrm{s}} = \rho_0^{\mathrm{s}} = \text{constant}$, it is possible to conclude from mass-conservation of the solid phase that

$$n = n(J) = 1 - J^{-1}(1 - n_0) \Rightarrow Jn(J) = J - (1 - n_0) \tag{72}$$

where n_0 is the initial value of the porosity corresponding to $J_0 = 1$. This is an exact result under the given assumptions.

Remark. A further simplification is obtained in the case it is assumed that the fluid is intrinsically incompressible as well, i.e. $\rho^{\mathrm{f}} = \rho_0^{\mathrm{f}} = \text{constant}$; then it is possible to cancel ρ^{f} from (71), which is rewritten as

$$\mathrm{d}_t J + \nabla_X \cdot \boldsymbol{W} = 0 \quad \text{in } \Omega_0 \times I \tag{73}$$

where we made use of the relation $\mathrm{d}_t(J\,n(J)) = \mathrm{d}_t(J - (1 - n_0)) = \mathrm{d}_t J$ from (72). □

What remains is to establish constitutive relations for $\boldsymbol{P}^{\mathrm{s}}(\boldsymbol{F})$ and $\boldsymbol{W}(\boldsymbol{F}, \boldsymbol{G})$, where $\boldsymbol{G} \overset{\text{def}}{=} \nabla_X p$ plays the role of "seepage resistance". In this prototype model we adopt the Neo-Hookean model for the solid skeleton and (a simplified version of) Darcy's law for the seepage:

$$\boldsymbol{P}^{\mathrm{s}}(\boldsymbol{F}) = 2GJ^{-\frac{2}{3}}\left[\boldsymbol{F} - \tfrac{1}{3} I_1(\boldsymbol{F})\boldsymbol{F}^{-\mathrm{T}}\right] + K\,J\,(J-1)\,\boldsymbol{F}^{-\mathrm{T}}, \tag{74}$$

$$\boldsymbol{W}(\boldsymbol{F}, \boldsymbol{G}) = -\boldsymbol{K} \cdot \boldsymbol{G}, \qquad \boldsymbol{K} = k[J - (1 - n_0)]\boldsymbol{C}^{-1}. \tag{75}$$

with $I_1 = \mathrm{tr}\left(\boldsymbol{F} \cdot \boldsymbol{F}^{\mathrm{T}}\right)$. We also assume intrinsic incompressibility of the solid particles (while the pore fluid can be compressible).

The fluid stress is given as

$$\boldsymbol{P}^{\mathrm{f}}(\boldsymbol{F}, p) = -p[J - (1 - n_0)]\boldsymbol{F}^{-\mathrm{T}} \tag{76}$$

and the constitutive law for the pore fluid is chosen as

$$\varrho^{\mathrm{f}}(p) = \varrho_0^{\mathrm{f}}\left(1 + \frac{p}{K^{\mathrm{f}}}\right). \tag{77}$$

We thus introduce the elastic constants G and K for the solid phase, the elastic constant K^{f} and the permeability constant k. As to the dependency on the independent fields $\boldsymbol{u}$ and p, we note that $J = J[\boldsymbol{u}]$ is a nonlinear differential operator in $\boldsymbol{u}$.

In summary, we have

$$-\boldsymbol{P}^{\mathrm{s}}(\boldsymbol{F}[\boldsymbol{u}]) \cdot \overleftarrow{\nabla}_X - \boldsymbol{P}^{\mathrm{f}}(\boldsymbol{F}[\boldsymbol{u}], p) \cdot \overleftarrow{\nabla}_X = \boldsymbol{0} \quad \text{in } \Omega_0 \times I, \tag{78}$$

$$\mathrm{d}_t \Phi[\boldsymbol{u}, p] + \nabla_X \cdot (\varrho^{\mathrm{f}}(p)\boldsymbol{W}(\boldsymbol{F}[\boldsymbol{u}], \boldsymbol{G}[p])) = 0 \quad \text{in } \Omega_0 \times I, \tag{79}$$

where we introduced the "conservation" property (conservation of total fluid mass)

$$\Phi[\boldsymbol{u}, p] \overset{\text{def}}{=} [J[\boldsymbol{u}] - (1 - n_0)]\,\varrho^{\mathrm{f}}(p). \tag{80}$$

The boundary conditions are given as

$$\boldsymbol{u} = \boldsymbol{u}_{\mathrm{p}} \qquad \text{on } \Gamma_{0,\mathrm{D}}^{(1)} \times I, \tag{81}$$

[11] This is in accordance with the classical mixture theory. The difference to the Porous Media Theory (PMT), advocated by DE BOER [1], is the expression for the fluid stress, which is $\boldsymbol{P}^{\mathrm{f}} = -pJ\boldsymbol{F}^{-\mathrm{T}}$ in the PMT.

$$\boldsymbol{t} \overset{\text{def}}{=} \boldsymbol{P}\cdot\boldsymbol{N} = \boldsymbol{t}_{\text{p}} \quad \text{on } \Gamma^{(1)}_{0,\text{N}} \times I, \tag{82}$$

$$p = p_{\text{p}} \quad \text{on } \Gamma^{(2)}_{0,\text{D}} \times I, \tag{83}$$

$$q \overset{\text{def}}{=} \boldsymbol{W}\cdot\boldsymbol{N} = q_{\text{p}} \quad \text{on } \Gamma^{(2)}_{0,\text{N}} \times I, \tag{84}$$

whereas the initial condition is chosen as

$$\Phi[\boldsymbol{u}_0,\, p_0] = n_0\varrho^{\text{f}}_0 \overset{\text{def}}{=} \hat{\varrho}^{\text{f}}_0. \tag{85}$$

For convenience, and without loss of generality, we may set $\boldsymbol{u}_0(\boldsymbol{X}) \overset{\text{def}}{=} \boldsymbol{u}(\boldsymbol{X}, t_0^-) = 0$ and $p_0(\boldsymbol{X}) \overset{\text{def}}{=} p(\boldsymbol{X}, t_0^-) = 0$.

4.2. Variational format in space–time

Using the generic format in Section 2, we may establish the spatially weak form, given in (1), as follows

$$a^{(\text{u})}(\boldsymbol{u},\, p;\, \delta\boldsymbol{u}) = l^{(\text{u})}(\delta\boldsymbol{u}), \tag{86}$$

$$(\text{d}_t\, \Phi[\boldsymbol{u},\, p],\, \delta p) + a^{(\text{p})}(\boldsymbol{u},\, p;\, \delta p) = l^{(\text{p})}(\delta p), \tag{87}$$

where we introduced the forms

$$\begin{aligned} a^{(\text{u})}(\boldsymbol{u},\, p;\, \delta\boldsymbol{u}) \;&=\; \int_{\Omega_0} (\delta\boldsymbol{u} \otimes \overleftarrow{\boldsymbol{\nabla}}_X) : \boldsymbol{P}(\boldsymbol{F},\, p)\, \text{d}\Omega_0 \\ &=\; \int_{\Omega_0} (\delta\boldsymbol{u} \otimes \overleftarrow{\boldsymbol{\nabla}}_X) :\, \left[\boldsymbol{P}^{\text{s}}(\boldsymbol{F}) + \boldsymbol{P}^{\text{f}}(\boldsymbol{F},\, p)\right] \text{d}\Omega_0, \end{aligned} \tag{88}$$

$$a^{(\text{p})}(\boldsymbol{u},\, p;\, \delta p) = \int_{\Omega_0} (\boldsymbol{\nabla}_X \delta p)\cdot \varrho^{\text{f}}(p)\boldsymbol{W}(\boldsymbol{F},\, \boldsymbol{G})\, \text{d}\Omega_0, \tag{89}$$

$$l^{(\text{u})}(\delta\boldsymbol{u}) = \int_{\Gamma^{(1)}_{0,\text{N}}} \delta\boldsymbol{u}\cdot\boldsymbol{t}_{\text{p}}\, \text{d}\Gamma_0, \tag{90}$$

$$l^{(\text{p})}(\delta p) = -\int_{\Gamma^{(2)}_{0,\text{N}}} \delta p\, q_{\text{p}}\, \text{d}\Gamma_0 \tag{91}$$

with $\boldsymbol{F} = \boldsymbol{F}[\boldsymbol{u}]$ and $\boldsymbol{G} = \boldsymbol{G}[p]$.

The forms $A_n(z;\, \delta z)$ and $L_n(z(t^-_{n-1});\, \delta z)$, given generically in (13) and (15), respectively, can thus be expanded as

$$A_n(z;\, \delta z) = \int_{I_n} \left[(\text{d}_t\, \Phi[z],\, \delta p) + a^{(\text{u})}(z;\, \delta\boldsymbol{u}) + a^{(\text{p})}(z;\, \delta p)\right] \text{d}t + \left(\Phi[z(t^+_{n-1})],\, \delta p(t^+_{n-1})\right), \tag{92}$$

$$L_n(z(t^-_{n-1});\, \delta z) = \int_{I_n} \left[l^{(\text{u})}(\delta\boldsymbol{u}) + l^{(\text{p})}(\delta p)\right] \text{d}t + (\Phi[z(t^-_{n-1})],\, \delta p(t^+_{n-1})), \tag{93}$$

where we used the abbreviation $z = (\boldsymbol{u},\, p)$. We may also derive the tangent form $A'_n(z;\, \delta z,\, \delta z^*)$ in the expanded form

$$\begin{aligned} A'_n(z;\, \delta z,\, \delta z^*) \;=\; & (\boldsymbol{\Phi}'_u[z(t^+_{n-1});\, \delta\boldsymbol{u}^*(t^+_{n-1})],\, \delta p(t^+_{n-1})) + (\Phi'_p[z(t^+_{n-1});\, \delta p^*(t^+_{n-1})],\, \delta p(t^+_{n-1})) \\ & + \int_{I_n} \left[(\text{d}_t(\boldsymbol{\Phi}'_u[z;\, \delta\boldsymbol{u}^*]),\, \delta p) + (\text{d}_t(\Phi'_p[z;\, \delta p^*]),\, \delta p)\right. \\ & + \left(a^{(\text{u})}\right)'_u (z;\, \delta\boldsymbol{u},\, \delta\boldsymbol{u}^*) + \left(a^{(\text{u})}\right)'_p (z;\, \delta\boldsymbol{u},\, \delta p^*) \\ & + \left.\left(a^{(\text{p})}\right)'_u (z;\, \delta p,\, \delta\boldsymbol{u}^*) + \left(a^{(\text{p})}\right)'_p (z;\, \delta p,\, \delta p^*)\right] \text{d}t, \end{aligned} \tag{94}$$

where we introduced the forms

$$(\boldsymbol{\Phi}'_u[z;\, \delta\boldsymbol{u}^*],\, \delta p) = \int_{\Omega_0} \delta p\varrho^{\text{f}}(p) J\boldsymbol{F}^{-\text{T}} :\, (\delta\boldsymbol{u}^* \otimes \overleftarrow{\boldsymbol{\nabla}}_X)\, \text{d}\Omega_0, \tag{95}$$

$$(\Phi'_p[z;\delta p^*],\delta p) = \int_{\Omega_0} \delta p[J-(1-n_0)]\frac{\mathrm{d}\varrho^{\mathrm{f}}(p)}{\mathrm{d}p}\delta p^*\,\mathrm{d}\Omega_0, \tag{96}$$

$$\left(a^{(\mathrm{u})}\right)'_u(z;\delta\boldsymbol{u},\delta\boldsymbol{u}^*) = \int_{\Omega_0}(\delta\boldsymbol{u}\otimes\overleftarrow{\boldsymbol{\nabla}}_X)\colon\left[\mathbf{L}^{\mathrm{s}}_a(\boldsymbol{F})+\mathbf{L}^{\mathrm{f}}_a(\boldsymbol{F},p)\right]\colon(\delta\boldsymbol{u}^*\otimes\overleftarrow{\boldsymbol{\nabla}}_X)\,\mathrm{d}\Omega_0, \tag{97}$$

$$\left(a^{(\mathrm{u})}\right)'_p(z;\delta\boldsymbol{u},\delta p^*) = -\int_{\Omega_0}(\delta\boldsymbol{u}\otimes\overleftarrow{\boldsymbol{\nabla}}_X)\colon[J-(1-n_0)]\boldsymbol{F}^{-\mathrm{T}}\delta p^*\,\mathrm{d}\Omega_0, \tag{98}$$

$$\left(a^{(\mathrm{p})}\right)'_u(z;\delta p,\delta\boldsymbol{u}^*) = -\int_{\Omega_0}(\boldsymbol{\nabla}_X\delta p)\cdot\varrho^{\mathrm{f}}(p)\mathcal{Y}_a(\boldsymbol{F},\boldsymbol{G})\colon(\delta\boldsymbol{u}^*\otimes\overleftarrow{\boldsymbol{\nabla}}_X)\,\mathrm{d}\Omega_0, \tag{99}$$

$$\begin{aligned}\left(a^{(\mathrm{p})}\right)'_p(z;\delta p,\delta p^*) \;=\; &-\int_{\Omega_0}(\boldsymbol{\nabla}_X\delta p)\cdot\boldsymbol{W}(\boldsymbol{F},\boldsymbol{G})\frac{\mathrm{d}\varrho^{\mathrm{f}}(p)}{\mathrm{d}p}\delta p^*\,\mathrm{d}\Omega_0\\ &+\int_{\Omega_0}(\boldsymbol{\nabla}_X\delta p)\cdot\varrho^{\mathrm{f}}(p)\boldsymbol{K}_a(\boldsymbol{F})\cdot(\boldsymbol{\nabla}_X\delta p^*)\,\mathrm{d}\Omega_0,\end{aligned} \tag{100}$$

where the assumption on an incompressible solid skeleton in (72) and the relation for the fluid stress in (76) were used. The algorithmic 4th order stiffness tensors $\mathbf{L}^{\mathrm{s}}_a$ and $\mathbf{L}^{\mathrm{f}}_a$, the 3rd order tensor $\mathcal{Y}_a$ and the 2nd order permeability tensor $\boldsymbol{K}_a$ are given via the relations

$$\left(\boldsymbol{P}^{\mathrm{s}}\right)'_u[\bullet;\delta\boldsymbol{u}] = \left(\boldsymbol{P}^{\mathrm{s}}\right)'_F:\delta\boldsymbol{F} = \mathbf{L}^{\mathrm{s}}_a\colon(\delta\boldsymbol{u}\otimes\overleftarrow{\boldsymbol{\nabla}}_X), \tag{101}$$

$$\left(\boldsymbol{P}^{\mathrm{f}}\right)'_u[\bullet;\delta\boldsymbol{u}] = \left(\boldsymbol{P}^{\mathrm{f}}\right)'_F:\delta\boldsymbol{F} = \mathbf{L}^{\mathrm{f}}_a\colon(\delta\boldsymbol{u}\otimes\overleftarrow{\boldsymbol{\nabla}}_X), \tag{102}$$

$$\boldsymbol{W}'_u[\bullet;\delta\boldsymbol{u}] = \boldsymbol{W}'_F:\delta\boldsymbol{F} = \mathcal{Y}_a\colon(\delta\boldsymbol{u}\otimes\overleftarrow{\boldsymbol{\nabla}}_X), \tag{103}$$

$$\boldsymbol{W}'_p[\bullet;\delta p] = \boldsymbol{W}'_G\cdot\delta\boldsymbol{G} = -\boldsymbol{K}_a\cdot(\boldsymbol{\nabla}_X\delta p). \tag{104}$$

For the specific choice of constitutive relations given in (74) and (75), i.e. the Neo-Hookean hyperelastic law for the solid skeleton and Darcy's permeability law for the fluid seepage, we obtain

$$\begin{aligned}\mathbf{L}^{\mathrm{s}}_a \;=\; &GJ^{-\frac{2}{3}}\left[\boldsymbol{I}\overline{\otimes}\boldsymbol{I}+\boldsymbol{F}\underline{\otimes}\boldsymbol{F}^{-1}+\frac{2}{9}I_1(\boldsymbol{F})\boldsymbol{F}^{-\mathrm{T}}\otimes\boldsymbol{F}^{-\mathrm{T}}-\frac{2}{3}\left(\boldsymbol{F}\otimes\boldsymbol{F}^{-\mathrm{T}}+\boldsymbol{F}^{-\mathrm{T}}\otimes\boldsymbol{F}\right)\right]\\ &+KJ(2J-1)\boldsymbol{F}^{-\mathrm{T}}\otimes\boldsymbol{F}^{-\mathrm{T}}-\boldsymbol{P}^{s}\underline{\otimes}\boldsymbol{F}^{-1},\end{aligned} \tag{105}$$

$$\mathbf{L}^{\mathrm{f}}_a = -p\left\{J\boldsymbol{F}^{-\mathrm{T}}\otimes\boldsymbol{F}^{-\mathrm{T}}-[J-(1-n_0)]\boldsymbol{F}^{-\mathrm{T}}\underline{\otimes}\boldsymbol{F}^{-1}\right\}, \tag{106}$$

$$\mathcal{Y}_a = -k\boldsymbol{G}\cdot\left\{J\boldsymbol{C}^{-1}\otimes\boldsymbol{F}^{-\mathrm{T}}-[J-(1-n_0)][\boldsymbol{C}^{-1}\underline{\otimes}\boldsymbol{F}^{-1}+\boldsymbol{F}^{-1}\overline{\otimes}\boldsymbol{C}^{-1}]\right\}, \tag{107}$$

$$\boldsymbol{K}_a = \boldsymbol{K} = k[J-(1-n_0)]\boldsymbol{C}^{-1}. \tag{108}$$

Finally, for the chosen constitutive model of the fluid compressibility (77), we obtain the constant derivative

$$\frac{\mathrm{d}\varrho^{\mathrm{f}}(p)}{\mathrm{d}p} = \frac{\varrho^{\mathrm{f}}_0}{K^{\mathrm{f}}}. \tag{109}$$

4.3. Space–time finite element format of primary problem

Upon employing the dG(0)-method, we introduce the finite element spaces ${}^{n}\mathbb{V}_h = {}^{n}\mathbb{U}_h\times{}^{n}\mathbb{P}_h$ associated with the time interval I_n. The FE-problem thus reads: For $n=1,2,\ldots,N$, find ${}^{n}z_h = ({}^{n}\boldsymbol{u}_h,{}^{n}p_h)\in{}^{n}\mathbb{V}_h$ such that

$$R^{(\mathrm{u})}_n({}^{n}z_h;\delta\boldsymbol{u}_h) = \Delta t\left[\langle l^{(\mathrm{u})}(\delta\boldsymbol{u}_h)\rangle_n - a^{(\mathrm{u})}({}^{n}z_h;\delta\boldsymbol{u}_h)\right] = 0,\quad \forall\delta\boldsymbol{u}_h\in{}^{n}\mathbb{U}^0_h, \tag{110}$$

$$\begin{aligned}R^{(\mathrm{p})}_n({}^{n}z_h;\delta p_h) \;=\; &\Delta t\left[\langle l^{(\mathrm{p})}(\delta p_h)\rangle_n - a^{(\mathrm{p})}({}^{n}z_h;\delta p_h)\right]-(\Phi[{}^{n}z_h]\\ &-\Phi[{}^{n-1}z_h],\delta p_h) = 0,\quad \forall\delta p_h\in{}^{n}\mathbb{P}^0_h,\end{aligned} \tag{111}$$

or

$$\Delta t\, a^{(\mathrm{u})}({}^n z_h;\, \delta \boldsymbol{u}_h) = \Delta t\, \langle l^{(\mathrm{u})}(\delta \boldsymbol{u}_h)\rangle_n, \quad \forall \delta \boldsymbol{u}_h \in {}^n\mathbb{U}_h^0, \tag{112}$$

$$(\Phi[{}^n z_h],\, \delta p_h) + \Delta t a^{(\mathrm{p})}({}^n z_h;\, \delta p_h) = (\Phi[{}^{n-1} z_h],\, \delta p_h) + \Delta t\, \langle l^{(\mathrm{p})}(\delta p_h)\rangle_n, \quad \forall \delta p_h \in {}^n\mathbb{P}_h^0. \tag{113}$$

A Newton step then becomes: Find $\mathrm{d}z_h = (\mathrm{d}\boldsymbol{u}_h, \mathrm{d}p_h) \in {}^n\mathbb{V}_h^0$ such that

$$\Delta t \left(a^{(\mathrm{u})}\right)'_u ({}^n z_h^{(l)};\, \delta \boldsymbol{u}_h, \mathrm{d}\boldsymbol{u}_h) + \Delta t \left(a^{(\mathrm{u})}\right)'_p ({}^n z_h^{(l)};\, \delta \boldsymbol{u}_h, \mathrm{d}p_h) = R_n^{(\mathrm{u})}({}^n z_h^{(l)};\, \delta \boldsymbol{u}_h), \quad \forall \delta \boldsymbol{u}_h \in {}^n\mathbb{U}_h^0, \tag{114}$$

$$\begin{aligned}&(\boldsymbol{\Phi}'_u[{}^n z_h^{(l)};\, \mathrm{d}\boldsymbol{u}_h],\, \delta p_h) + (\Phi'_p[{}^n z_h^{(l)};\, \mathrm{d}p_h],\, \delta p_h) + \Delta t \left(a^{(\mathrm{p})}\right)'_u ({}^n z_h^{(l)};\, \delta p_h, \mathrm{d}\boldsymbol{u}_h)\\ &\quad + \Delta t \left(a^{(\mathrm{p})}\right)'_p ({}^n z_h^{(l)};\, \delta p_h, \mathrm{d}p_h) = R_n^{(\mathrm{p})}({}^n z_h^{(l)};\, \delta p_h), \quad \forall \delta p_h \in {}^n\mathbb{P}_h^0.\end{aligned} \tag{115}$$

4.4. Error computation and the dual problem

We shall assume that the dG(0)-method is used to compute the primary solution $z_h = (\boldsymbol{u}_h,\, p_h)$ and that the appropriate dual solution $z^* = (\boldsymbol{u}^*,\, p^*)$ has been found, whereby $\boldsymbol{u}^*(\boldsymbol{X}, t)$ is the dual displacement and $p^*(\boldsymbol{X}, t)$ is the dual excess pore pressure. We may then use the error representation in (48) and (49) directly to obtain

$$\begin{aligned}R_n(z_h;\, z^*) = \Delta t\Big[&\langle l^{(\mathrm{u})}(\boldsymbol{u}^*)\rangle_n + \langle l^{(\mathrm{p})}(p^*)\rangle_n - a^{(\mathrm{u})}({}^n z_h;\, \langle \boldsymbol{u}^*\rangle)\\ &- a^{(\mathrm{p})}({}^n z_h;\, \langle p^*\rangle)\Big] - (\Phi[{}^n z_h] - \Phi[{}^{n-1} z_h],\, p^*(t_{n-1}^+)).\end{aligned} \tag{116}$$

As to the explicit solution of the dual solution, it is given by (48), whereby A_n^* and L_n^* can be expanded as

$$\begin{aligned}A_n^*(z;\, \delta z^*,\, z^*) = \int_{I_n} \Big[&-(\boldsymbol{\Phi}'_u[z;\, \delta \boldsymbol{u}^*],\, \mathrm{d}_t p^*) + (\Phi'_p[z;\, \delta p^*],\, \mathrm{d}_t p^*)\\ &+ \left(a^{(\mathrm{u})}\right)'_u (z;\, \boldsymbol{u}^*,\, \delta \boldsymbol{u}^*) + \left(a^{(\mathrm{u})}\right)'_p (z;\, \boldsymbol{u}^*,\, \delta p^*)\\ &+ \left(a^{(\mathrm{p})}\right)'_u (z;\, p^*,\, \delta \boldsymbol{u}^*) + \left(a^{(\mathrm{p})}\right)'_p (z;\, p^*,\, \delta p^*)\Big]\, \mathrm{d}t\\ &+ (\boldsymbol{\Phi}'_u[z(t_n^-);\, \delta \boldsymbol{u}^*(t_n^-)],\, p^*(t_n^-)) + (\Phi'_p[z(t_n^-);\, \delta p^*(t_n^-)],\, p^*(t_n^-)),\end{aligned} \tag{117}$$

$$L_N^*(z;\, \delta z^*) = \bar{Q}'_u(z(t_N^-);\, \delta \boldsymbol{u}^*(t_N^-)) + \bar{Q}'_p(z(t_N^-);\, \delta p^*(t_N^-)) + Q'_{u,N}(z;\, \delta \boldsymbol{u}^*) + Q'_{p,N}(z;\, \delta p^*) \tag{118}$$

$$\begin{aligned}L_n^*(z;\, \delta z^*,\, z^*(t_n^+)) = &(\boldsymbol{\Phi}'_u[z(t_n^-);\, \delta \boldsymbol{u}^*(t_n^-)],\, p^*(t_n^+)) + (\Phi'_p[z(t_n^-);\, \delta p^*(t_n^-)],\, p^*(t_n^+))\\ &+ Q'_{u,n}(z;\, \delta \boldsymbol{u}^*) + Q'_{p,n}(z;\, \delta p^*), \quad n < N\end{aligned} \tag{119}$$

5. Numerical examples

We shall illustrate the sequential-adaptive strategy by computing the response of a partially saturated "sponge",[12] adopting the poro-hyper-elastic formulation described in the previous section. We normalize the problem with respect to the shear stiffness G, the permeability constant k and the length a. Doing so, we define the dimensionless variables representing the prescribed vertical load (traction) traction, $\bar{T}_{\mathrm{p}}$, the elastic bulk modulus, $\bar{K}$, the fluid compressibility, $\bar{K}^{\mathrm{f}}$, the spatial position, $\bar{\boldsymbol{X}}$, and the time, $\bar{t}$, as follows:

$$\bar{T}_{\mathrm{p}} \overset{\mathrm{def}}{=} \frac{1}{G} T_{\mathrm{p}}, \tag{120}$$

[12] The notion of a sponge is adopted to illustrate the poro-mechanics behavior in large deformation elasticity. Note that for applications to, e.g., geo-mechanics problems, the modeling of the solid skeleton would preferably be that of elasto–(visco-)plasticity.

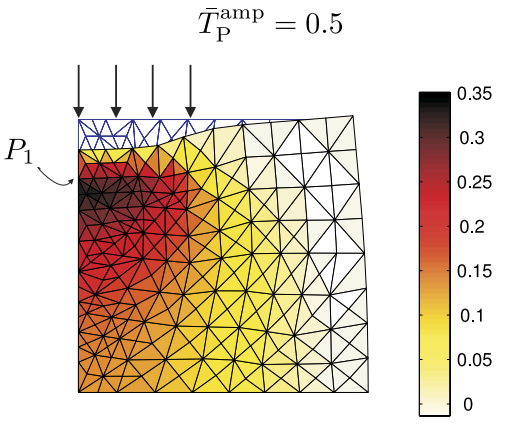

Fig. 4. Problem description: "Sponge" of size $5a \times 5a$ subjected to vertical loading $\bar{T}_{\mathrm{p}}$. The actual deformation at time $\bar{t} = 0.1$ is shown for $\bar{T}_{\mathrm{p}}^{\mathrm{amp}} = 0.5$.

$$\bar{K} \overset{\text{def}}{=} \frac{1}{G}K, \qquad \bar{K}^{\mathrm{f}} \overset{\text{def}}{=} \frac{1}{G}K^{\mathrm{f}}, \tag{121}$$

$$\bar{\boldsymbol{X}} \overset{\text{def}}{=} \frac{1}{a}\boldsymbol{X}, \qquad \bar{t} \overset{\text{def}}{=} \frac{2kG}{a^2}t. \tag{122}$$

The dimensionless material data used in the computations are $\bar{K} = 3/2$, corresponding to Poisson's ratio $\nu = 0$ for the linear response, and $\bar{K}^{\mathrm{f}} = 10^3$, corresponding to a nearly incompressible fluid.

Fig. 4 shows a 2D domain of size $5a \times 5a$ that is studied under time-dependent loading in terms of a constant vertical traction distributed on the upper surface over the spatial length $2a$. The left and lower boundaries are subjected to symmetry boundary conditions, while the top and right boundaries are free. In particular, the point of interest P_1 at $\boldsymbol{X}_1$ (located on the left boundary at a depth of $0.5a$ below the surface) is indicated in the Figure. The non-dimensional loading is applied in terms of a ramp-function in time

$$\bar{T}_{\mathrm{P}}(t) = \begin{cases} \dfrac{\bar{t}}{\bar{t}_{\mathrm{r}}}\bar{T}_{\mathrm{P}}^{\mathrm{amp}} & 0 < \bar{t} < \bar{t}_{\mathrm{r}} \\ \bar{T}_{\mathrm{P}}^{\mathrm{amp}} & \bar{t}_{\mathrm{r}} < \bar{t}, \end{cases} \tag{123}$$

where $\bar{t}_{\mathrm{r}}$ is the duration of the ramp and $\bar{T}_{\mathrm{p}}^{\mathrm{amp}}$ is the non-dimensional amplitude. Subsequently, we choose $\bar{t}_{\mathrm{r}} = 0.01$ throughout.

We shall now study the accuracy of the pressure at point P_1 and time $\bar{t} = 0.1$. To this end, we conduct a simulation up until the time of interest, i.e. the non-dimensional end time is $\bar{T} = 0.1$, and we choose the goal quantity

$$Q(\boldsymbol{u}, p)\left[= \bar{Q}(\boldsymbol{u}(\bar{T}), p(\bar{T}))\right] = p(\bar{\boldsymbol{X}}_1, \bar{T}). \tag{124}$$

Following the arguments presented in, e.g., Larsson and Runesson [25], we choose to regularize this measure in space and time by introducing the slightly modified goal quantity

$$Q(\boldsymbol{u}, p) = \frac{\int_{\Omega\times I} \psi(\bar{\boldsymbol{X}}, \bar{t})\, p(\bar{\boldsymbol{X}}, \bar{t})\, \mathrm{d}\Omega \times \mathrm{d}\bar{t}}{\int_{\Omega\times I} \psi(\bar{\boldsymbol{X}}, \bar{t})\, \mathrm{d}\Omega \times \mathrm{d}\bar{t}}. \tag{125}$$

The weight (or mollifier) function can be multiplicatively decomposed into spatial and temporal weights as follows:

$$\psi(\bar{\boldsymbol{X}}, \bar{t}) \overset{\text{def}}{=} \psi_\Omega(\bar{\boldsymbol{X}})\psi_I(\bar{t}), \qquad \psi_\Omega = \begin{cases} 1 & \|\bar{\boldsymbol{X}} - \bar{\boldsymbol{X}}_1\| \le r_\Omega \\ 0 & \|\bar{\boldsymbol{X}} - \bar{\boldsymbol{X}}_1\| > r_\Omega \end{cases}, \qquad \psi_I = \begin{cases} 1 & \bar{t} > \bar{T} - r_I \\ 0 & \bar{t} < \bar{T} - r_I, \end{cases} \tag{126}$$

where the radii of influence[13] are chosen as $r_\Omega = 0.1$ and $r_I = 0.001$.

[13] The radii r_Ω and r_I represent the area in space and time, respectively, over which the pressure is evaluated in the mean sense.

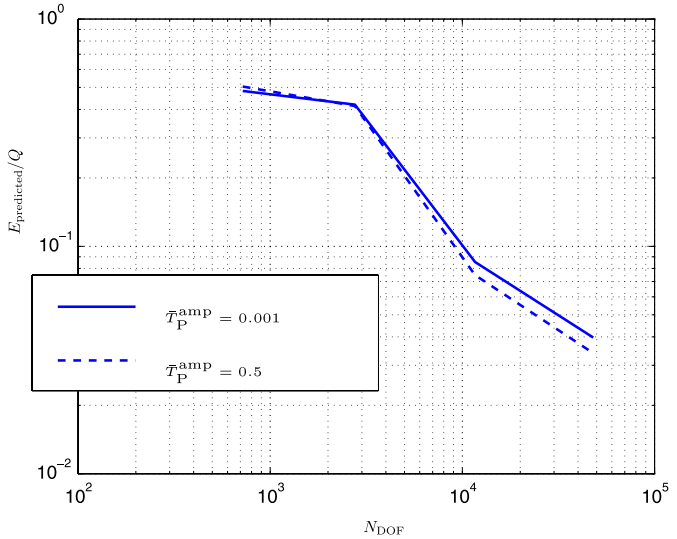

Fig. 5. Convergence of predicted error for uniform space–time refinement. $\bar{T}_{\text{P}}^{\text{amp}} = 0.001$ corresponds to (nearly) linear response, whereas $\bar{T}_{\text{P}}^{\text{amp}} = 0.5$ corresponds to strongly non-linear response.

Remark. The construction of Q is chosen such that, when using the same quadrature for the two integrals, a constant is evaluated exactly, independent of the quadrature. □

Fig. 5 shows the convergence of the predicted error with increasing number of space–time degrees of freedom, N_{DOF}, for uniform refinement in space and time. The corresponding effectivity of the error estimation is shown in Fig. 6 in terms of the effectivity index,

$$\eta \overset{\text{def}}{=} \frac{E_{\text{predicted}}}{E_{\text{true}}}, \tag{127}$$

where $E_{\text{predicted}} = R(z_h^{\text{SOL}}; \tilde{z}^*)$ as presented in Eq. (66), and the true error E_{true} can be computed using an overkill solution for $(\boldsymbol{u}, p)$. Here, the dual solution is computed on the same mesh (using a hierarchically refined discretization) as that of the primal problem for each analysis. The results are shown for (nearly) linear response (with $\bar{T}_{\text{P}}^{\text{amp}} = 0.001$) as well as for strongly non-linear response (with $\bar{T}_{\text{P}}^{\text{amp}} = 0.5$).

Next, we study the performance of the suggested time-sequential adaptive strategy. To this end, we consider the nonlinear case, defined by $\bar{T}_{\text{P}}^{\text{amp}} = 0.5$, and choose to study the long-time effect of consolidation in the problem by running the simulation for a longer time by setting $\bar{T} = 1.0$. We shall now consider two different goal functions, defined by $i = 1$ and $i = 2$, as follows:

$$Q_i(\boldsymbol{u}, p) = \frac{\int_{\Omega\times I} \psi_i(\bar{\boldsymbol{X}}, \bar{t})\, p(\bar{\boldsymbol{X}}, \bar{t})\, \mathrm{d}\Omega \times \mathrm{d}\bar{t}}{\int_{\Omega\times I} \psi(\bar{\boldsymbol{X}}, \bar{t})\, \mathrm{d}\Omega \times \mathrm{d}\bar{t}}, \quad i = 1, 2 \tag{128}$$

where the weights are defined by

$$\begin{aligned} &\psi_i(\bar{\boldsymbol{X}}, \bar{t}) \overset{\text{def}}{=} \psi_\Omega(\bar{\boldsymbol{X}})\psi_{I,i}(\bar{t}), \qquad \psi_\Omega = \begin{cases} 1 & \|\bar{\boldsymbol{X}} - \bar{\boldsymbol{X}}_1\| \le r_\Omega \\ 0 & \|\bar{\boldsymbol{X}} - \bar{\boldsymbol{X}}_1\| > r_\Omega \end{cases}, \\ &\psi_{I,i} = \begin{cases} 1 & \bar{t} > \bar{T} - r_{I,i} \\ 0 & \bar{t} < \bar{T} - r_{I,i} \end{cases}, \quad i = 1, 2. \end{aligned} \tag{129}$$

The spatial averaging radius is $r_\Omega = 0.1$ (like in the previous example), whereas the two different measures are distinguished by $r_{I,1} = 0.001$ and $r_{I,2} = 0.5$, respectively, in the temporal domain. Hence, the difference lies in the temporal averaging, i.e., Q_1 represents the pressure at the end time $\bar{t} = \bar{T} = 1.0$ in a regularized sense, while the Q_2 represents the mean pressure during the second half of the time interval. We compare the convergence of the predicted

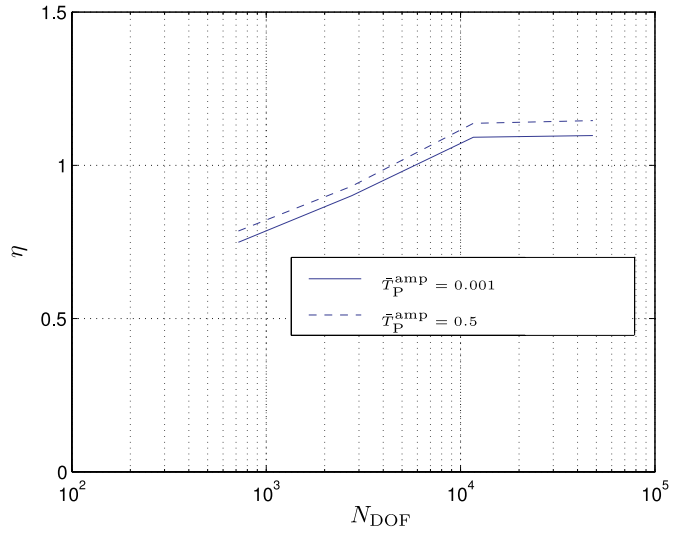

Fig. 6. Convergence of effectivity of the error estimator for uniform space–time refinement.

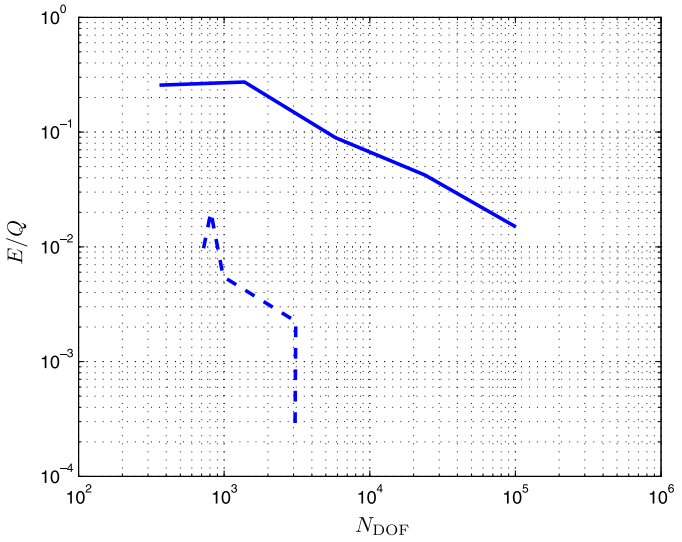

Fig. 7. Convergence of predicted error in Q_1 for uniform (solid line) and time-sequentially adaptive (dashed line) space–time refinement.

error for the time-sequential adaptive strategy to that of a uniform space–time refinement for Q_1 and Q_2 in Figs. 7 and 8, respectively. In these examples, the background dual solution is that computed on the initial mesh.

Remark. N_{DOF} is the total number of degrees of freedom in space–time. The rate of convergence depends strongly on the "ratio" for refining in space versus time. □

Next, we shall study the resulting space–time meshes for the adaptive strategy, aiming at equi-balanced error contributions from the spatial and temporal discretization and a total relative error that does not exceed the tolerance $TOL = 0.5\%$. The initial mesh is composed of 5 equal time steps and $N_{\mathrm{DOF}}^{\mathrm{space}} = 138$ spatial degrees of freedom on each time-slab. In Figs. 9 and 10, the resulting time-mesh function, defined as the time-step length $\Delta\bar{t}$ as a function of time, is shown for the quantities Q_1 and Q_2, respectively. Figs. 11 and 12 show the resulting space-mesh function, defined as $N_{\mathrm{DOF}}^{\mathrm{space}}$ versus time. Finally, Figs. 13 and 14 show a series of snapshots of the spatial mesh at $\bar{t} = 0.1, 0.5$ and 1.0 for the two different goal quantities.

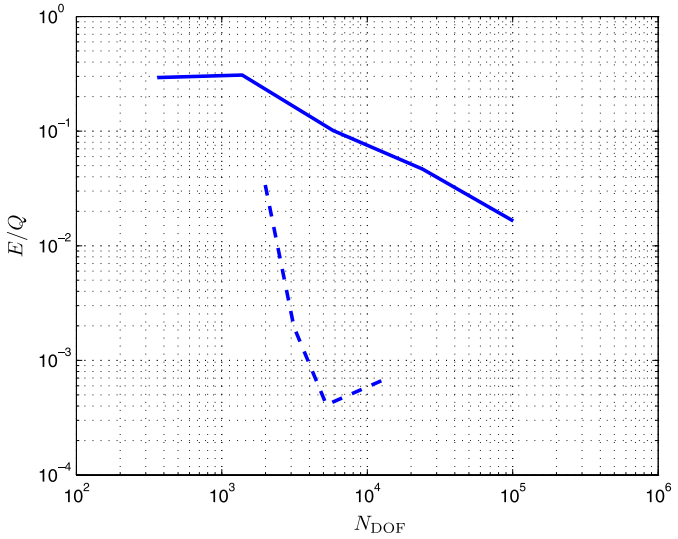

Fig. 8. Convergence of predicted error in Q_2 for uniform (solid line) and time-sequentially adaptive (dashed line) space–time refinement.

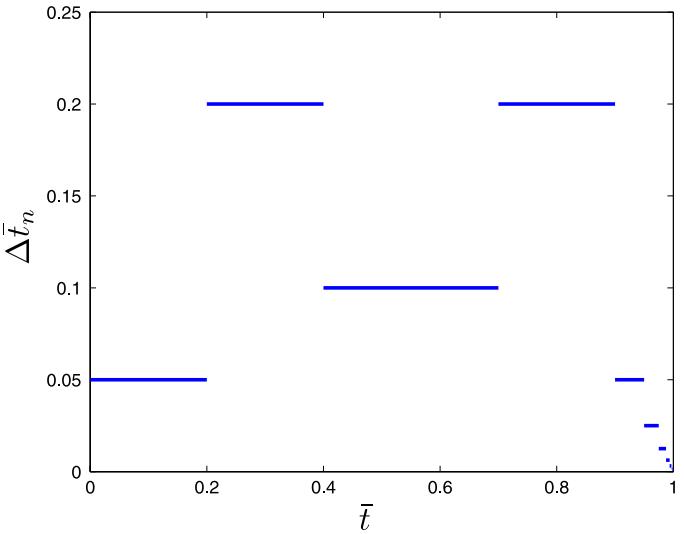

Fig. 9. The resulting time-mesh function from the time-sequential adaptive strategy for the goal-quantity Q_1, showing the development of the time-step length $\Delta\bar{t}$ with time.

6. Concluding remarks and future work

In this paper we have proposed a novel sequential-adaptive space–time finite element method for the coupled consolidation problem. This strategy is particularly suitable for linear goal functionals (such as the mean value of the pore pressure over a chosen finite time interval), in which case the dual loading is independent of the primal solution (and its approximation). In such cases it offers considerable advantages over the full-fledged concurrent adaptive strategy. Clearly, the present problem of poro-elasticity is too simple to provide an "acid test" for the significance of computing the dual solution accurately away from the end-time. The reason is that this problem has "parabolic character", so that errors are strongly damped, cf. also below.

As to future developments, the accuracy of the error prediction with respect to the choice of the background (initial) space–time mesh should be investigated. Our purpose is also to increase the physical realism by including material nonlinearities in the model, e.g. in terms of plasticity and viscoplasticity. Since it is sufficient to solve a suitably linearized dual problem, it is believed that the present approach will demonstrate its competitiveness when

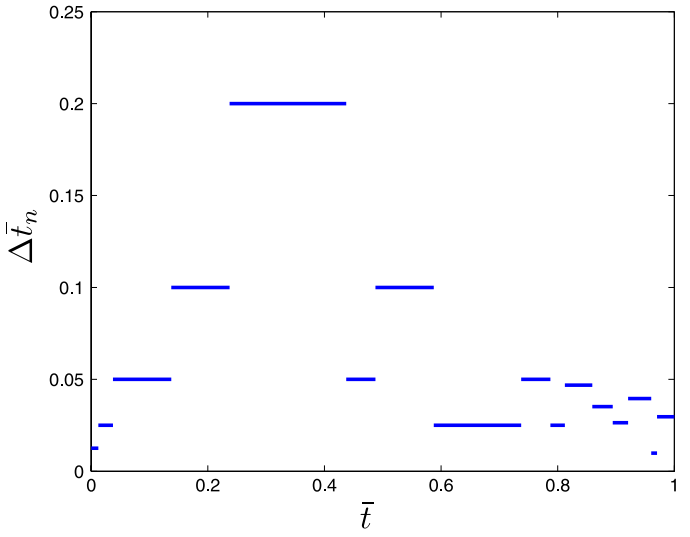

Fig. 10. The resulting time-mesh function from the time-sequential adaptive strategy for the goal-quantity Q_2, showing the development of the time-step length $\Delta\bar{t}$ with time.

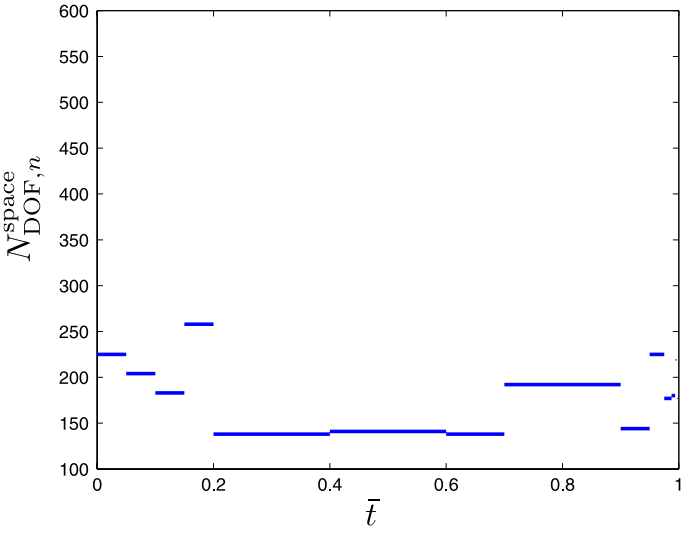

Fig. 11. The resulting space-mesh function from the time-sequential adaptive strategy for the goal-quantity Q_1, showing the development of the number of spatial degrees of freedom in the mesh, $N^{\text{space}}_{\text{DOF}}$, with time.

nonlinearities are incorporated. Moreover, dynamics (inertia terms) will be included, which are significant for road and railway mechanics problems subjected to traffic loading. For such problems it becomes obvious that it is necessary to solve the dual problem globally in time in an accurate fashion in order to appropriately account for the transport of error in space–time.

Appendix A. Matrix format of primal problem — generic format

We introduce the basis functions ${}^nN_i(\boldsymbol{X})$ in ${}^n\mathbb{V}_h$, such that ${}^nz_h = \sum_{i=1}^{M_n} {}^nN_i({}^n\underline{Z})_i$, with ${}^n\underline{Z} = [{}^nZ_1, \ldots, {}^nZ_{M_n}]^{\mathrm{T}}$ as the vector of M_n unknowns in time step n. In matrix notation, we may now rewrite (33) as that of finding $\mathrm{d}z_h = \sum_{i=1}^{M_n} {}^nN_i(\mathrm{d}\underline{Z})_i$ from

$$ {}^n\underline{K}^{(l)}\mathrm{d}\underline{Z} = {}^n\underline{r}^{(l)} \quad \text{with } {}^n\underline{K} \overset{\text{def}}{=} {}^n\underline{B} + \Delta t_n\, {}^n\underline{A} \tag{A.1}$$

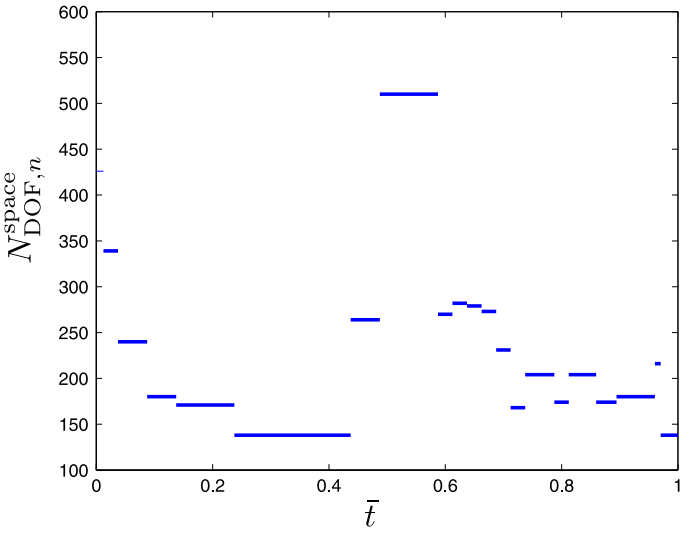

Fig. 12. The resulting space-mesh function from the time-sequential adaptive strategy for the goal-quantity Q_2, showing the development of the number of spatial degrees of freedom in the mesh, $N_{\mathrm{DOF}}^{\mathrm{space}}$, with time.

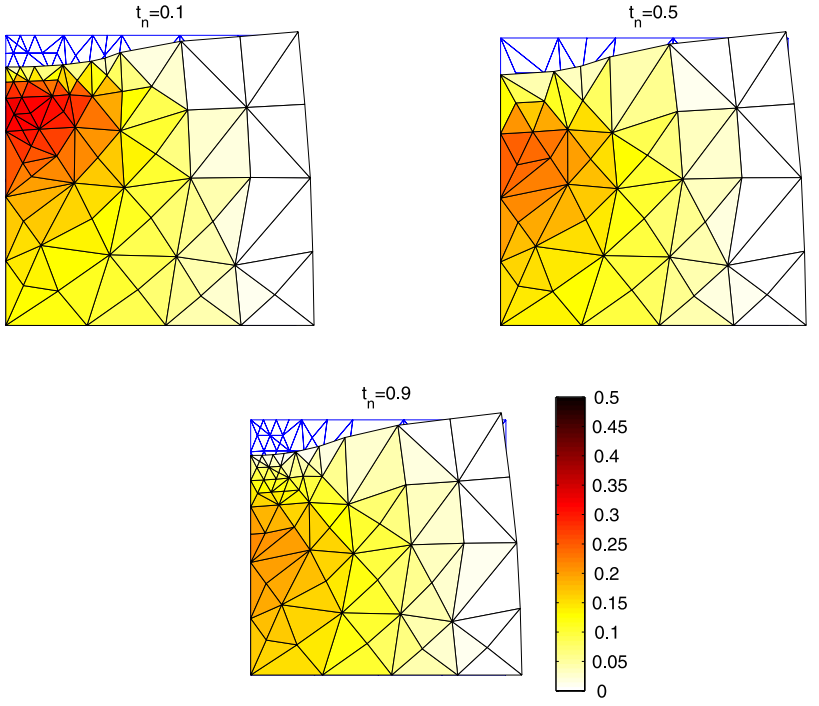

Fig. 13. Snapshots of the resulting spatial meshes at times $\bar{t} = 0.1$, 0.5 and 1.0 for the goal-quantity Q_1.

where the introduced matrices are defined as

$$\left({}^{n+1,n}\underline{B}\right)_{ij} = \left(\Phi'[{}^{n}z_h, {}^{n}N_j], {}^{n+1}N_i\right) = ({}^{n+1}N_i, \Phi'[{}^{n}z_h, {}^{n}N_j]), \quad \underline{B} \overset{\text{def}}{=} {}^{n,n}\underline{B} \tag{A.2}$$

$$\left({}^{n}\underline{A}\right)_{ij} = a'({}^{n}z_h; {}^{n}N_i, {}^{n}N_j) \tag{A.3}$$

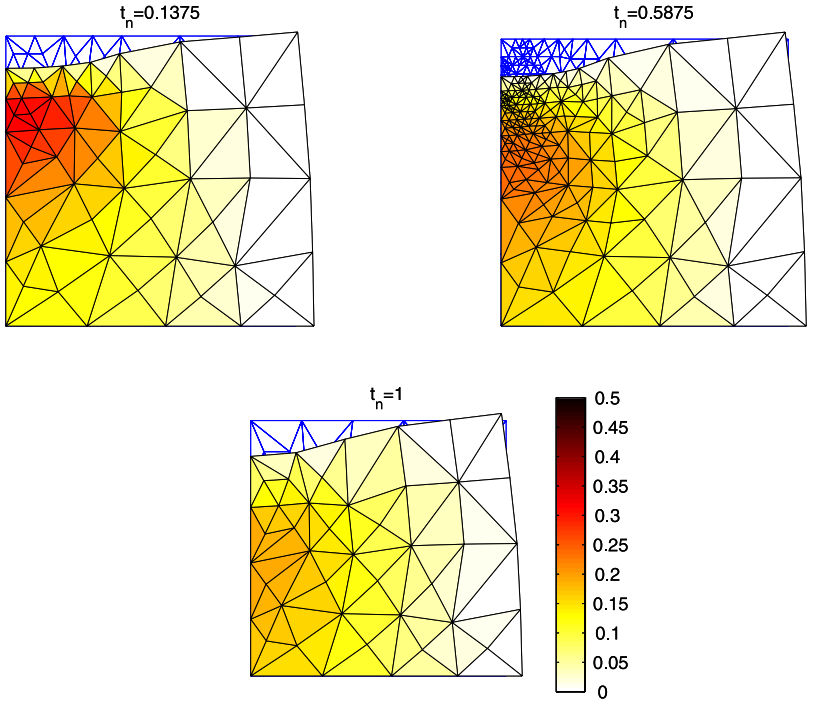

Fig. 14. Snapshots of the resulting spatial meshes at times $\bar{t} = 0.1$, 0.5 and 1.0 for the goal-quantity Q_2.

$$\begin{aligned} \left({}^{n}\underline{r}\right)_i &= R({}^{n}z_h; {}^{n}N_i) \\ &= \Delta t \left(\langle l({}^{n}N_i)\rangle_n - a({}^{n}z_h; {}^{n}N_i)\right) - \left(\Phi[{}^{n}z_h] - \Phi[{}^{n-1}z_h], {}^{n}N_i\right). \end{aligned} \tag{A.4}$$

Note that the generic coefficient matrix, introduced as $\underline{K} \overset{\text{def}}{=} \underline{B} + \Delta t\,\underline{A}$, is generally non-symmetrical, in particular because of the non-symmetry that is normally embedded in $\underline{B}$.

Appendix B. Matrix format of dual problem — generic format

Upon inserting ${}^{n}z_h^* = \sum_{i=1}^{M_n} {}^{n}N_i({}^{n}\underline{Z}^*)_i \in {}^{n}\mathbb{V}_h^0$ into (55), we obtain

$$({}^{n}\underline{K})^{\mathrm{T}\,n}\underline{Z}^* = ({}^{n+1,n}\underline{B})^{\mathrm{T}\,n+1}\underline{Z}^* + {}^{n}\underline{Q}, \quad n < N \tag{B.1}$$

where the matrices ${}^{n+1,n}\underline{B}$ and ${}^{n}\underline{A}$ where defined in (A.2) and (A.3), whereas

$$({}^{n}\underline{Q})_i = Q_n'({}^{n}z_h; {}^{n}N_i). \tag{B.2}$$

The adjoint character of (B.1) to the primary problem in (A.1) becomes apparent.

Remark. In the first step, $n = N$, we compute ${}^{N}\underline{Z}^*$ from the equation

$${}^{N}\underline{K}^{\mathrm{T}\,N}\underline{Z}^* = {}^{N}\underline{Q} \quad \text{with } ({}^{N}\underline{Q})_i = \bar{Q}'({}^{N}z_h; {}^{N}N_i) + Q_N'({}^{N}z_h; {}^{N}N_i). \tag{B.3}$$

As pointed out above, the "initial value" ${}^{N+1}\underline{Z}^*$may not even exist. However, if it does exist it can be computed from the relation

$$\left({}^{N+1,N}\underline{B}\right)^{\mathrm{T}}\,{}^{N+1}\underline{Z}^* = {}^{N}\underline{\bar{Q}}, \quad \text{with } ({}^{N}\underline{\bar{Q}})_i = \bar{Q}'({}^{N}z_h; {}^{N}N_i). \quad \square \tag{B.4}$$

Appendix C. Matrix format of primal problem — consolidation

We now introduce the basis functions ${}^n\boldsymbol{N}_i^{(\mathrm{u})}(\boldsymbol{X})$ in ${}^n\mathbb{U}_h$ and ${}^nN_i^{(\mathrm{p})}(\boldsymbol{X})$ in ${}^n\mathbb{P}_h$ such that

$$ {}^n\boldsymbol{u}_h = \sum_{i=1}^{M_n^{(\mathrm{u})}} {}^n\boldsymbol{N}_i^{(\mathrm{u})}({}^n\underline{U})_i, \qquad {}^np_h = \sum_{i=1}^{M_n^{(\mathrm{p})}} {}^nN_i^{(\mathrm{p})}({}^n\underline{P})_i, \tag{C.1} $$

are matrix representations, whereby ${}^n\underline{U}$ and ${}^n\underline{P}$ are column vectors of $M_n^{(\mathrm{u})}$ and $M_n^{(\mathrm{p})}$ unknowns, respectively, in the time interval I_n. In matrix notation, we may now rewrite the system (114) and (115) as that of computing $\mathrm{d}\boldsymbol{u}_h = \sum_{i=1}^{M_n^{(\mathrm{u})}} {}^n\boldsymbol{N}_i^{(\mathrm{u})}(\mathrm{d}\underline{U})_i$ and $\mathrm{d}p_h = \sum_{i=1}^{M_n^{(\mathrm{p})}} {}^nN_i^{(\mathrm{p})}(\mathrm{d}\underline{P})_i$ from

$$ \begin{bmatrix} \Delta t\, {}^n\underline{S} & \Delta t\, {}^n\underline{C}_1 \\ {}^n\underline{C}_3 + \Delta t\, {}^n\underline{C}_2 & {}^n\underline{M} + \Delta t\, {}^n\underline{K} \end{bmatrix} \begin{bmatrix} \mathrm{d}\underline{U} \\ \mathrm{d}\underline{P} \end{bmatrix} = \begin{bmatrix} {}^n\underline{r}^{(\mathrm{u})} \\ {}^n\underline{r}^{(\mathrm{p})} \end{bmatrix}, \tag{C.2} $$

where the introduced matrices are defined via the component identities

$$ ({}^n\underline{S})_{ij} = (a^{(\mathrm{u})})'_u({}^nz_h; {}^n\boldsymbol{N}_i^{(\mathrm{u})}, {}^n\boldsymbol{N}_j^{(\mathrm{u})}) \tag{C.3} $$

$$ ({}^n\underline{C}_1)_{ij} = (a^{(\mathrm{u})})'_p({}^nz_h; {}^n\boldsymbol{N}_i^{(\mathrm{u})}, {}^nN_j^{(\mathrm{p})}) \tag{C.4} $$

$$ ({}^n\underline{C}_2)_{ij} = (a^{(\mathrm{p})})'_u({}^nz_h; {}^nN_i^{(\mathrm{p})}, {}^n\boldsymbol{N}_j^{(\mathrm{u})}) \tag{C.5} $$

$$ ({}^n\underline{K})_{ij} = (a^{(\mathrm{p})})'_p({}^nz_h; {}^nN_i^{(\mathrm{p})}, {}^nN_j^{(\mathrm{p})}) \tag{C.6} $$

$$ ({}^n\underline{C}_3)_{ij} = (\Phi'_u[{}^nz_h; {}^n\boldsymbol{N}_j^{(\mathrm{u})}], {}^nN_i^{(\mathrm{p})}) \tag{C.7} $$

$$ ({}^n\underline{M})_{ij} = (\Phi'_p[{}^nz_h; {}^n\boldsymbol{N}_j^{(p)}], {}^nN_i^{(\mathrm{p})}) \tag{C.8} $$

$$ ({}^n\underline{r}(\mathrm{u}))_i = R^{(\mathrm{u})}({}^nz_h; {}^n\boldsymbol{N}_i^{(\mathrm{u})}) \tag{C.9} $$

$$ ({}^n\underline{r}(\mathrm{p}))_i = R^{(\mathrm{p})}({}^nz_h; {}^nN_i^{(\mathrm{p})}). \tag{C.10} $$

Remark. In the special case of fluid incompressibility, $\varrho^{\mathrm{f}} = \varrho_0^{\mathrm{f}} =$ constant, then $K^{\mathrm{f}} = \infty$ and $(\Phi'_p[z; \delta p^*], \delta p) = 0$, i.e. $\underline{M} = \underline{0}$. Since all integrals involving K^{f} vanish, this means that $\underline{K}$ becomes symmetrical (with the present choice of seepage model).

Appendix D. Matrix format of dual problem — consolidation

The FE-solution of z^*, denoted by z_h^*, is obtained directly from the generic formulation in Section 2.4. For example, in the case the dG(0)-method is used, we may directly identify from (B.1), with

$$ {}^n\boldsymbol{u}_h^* = \sum_{i=1}^{M_n^{(\mathrm{u})}} {}^n\boldsymbol{N}_i^{(\mathrm{u})}({}^n\underline{U}^*)_i, \qquad {}^np_h = \sum_{i=1}^{M_n^{(\mathrm{p})}} {}^nN_i^{(\mathrm{p})}({}^n\underline{P}^*)_i, \tag{D.1} $$

that $({}^n\underline{U}^*, {}^n\underline{P}^*)$ must satisfy the system

$$ \begin{bmatrix} \Delta t\, ({}^n\underline{S})^{\mathrm{T}} & ({}^n\underline{C}_3)^{\mathrm{T}} + \Delta t\, ({}^n\underline{C}_2)^{\mathrm{T}} \\ \Delta t\, ({}^n\underline{C}_1)^{\mathrm{T}} & ({}^n\underline{M})^{\mathrm{T}} + \Delta t\, ({}^n\underline{K})^{\mathrm{T}} \end{bmatrix} \begin{bmatrix} {}^n\underline{U}^* \\ {}^n\underline{P}^* \end{bmatrix} = \begin{bmatrix} ({}^{n+1,n}\underline{C}_3)^{\mathrm{T}\,n+1}\underline{P}^* + \Delta t\, {}^n\underline{Q}^{(\mathrm{u})} \\ ({}^{n+1,n}\underline{M})^{\mathrm{T}\,n+1}\underline{P}^* + \Delta t\, {}^n\underline{Q}^{(\mathrm{p})} \end{bmatrix}, \tag{D.2} $$

where ${}^n\underline{Q}^{(u)}$ and ${}^n\underline{Q}^{p}$ are column vectors defined by the identities

$$ ({}^n\underline{Q}^{(\mathrm{u})})_i = Q'_{u,n}({}^nz_h; {}^n\boldsymbol{N}_i^{(\mathrm{u})}), \tag{D.3} $$

$$ ({}^n\underline{Q}^{(\mathrm{p})})_i = Q'_{p,n}({}^nz_h; {}^nN_i^{(\mathrm{p})}). \tag{D.4} $$

In the first step, $n = N$, we obtain the problem

$$\begin{bmatrix} \Delta t\,({}^{N}\underline{S})^{\mathrm{T}} & ({}^{N}\underline{C}_3)^{\mathrm{T}} + \Delta t\,({}^{N}\underline{C}_2)^{\mathrm{T}} \\ \Delta t\,({}^{N}\underline{C}_1)^{\mathrm{T}} & ({}^{N}\underline{M})^{\mathrm{T}} + \Delta t\,({}^{N}\underline{K})^{\mathrm{T}} \end{bmatrix} \begin{bmatrix} {}^{N}\underline{U}^{*} \\ {}^{N}\underline{P}^{*} \end{bmatrix} = \begin{bmatrix} \Delta t\,{}^{N}\underline{Q}^{(\mathrm{u})} \\ \Delta t\,{}^{N}\underline{Q}^{(\mathrm{p})} \end{bmatrix}, \tag{D.5}$$

where

$$({}^{N}\underline{Q}^{(\mathrm{u})})_i = \bar{Q}'_u({}^{N}z_h;\, {}^{N}\boldsymbol{N}_i^{(\mathrm{u})}) + Q'_{u,N}({}^{N}z_h;\, {}^{N}\boldsymbol{N}_i^{(\mathrm{u})}), \tag{D.6}$$

$$({}^{N}\underline{Q}^{(\mathrm{p})})_i = \bar{Q}'_p({}^{N}z_h;\, {}^{N}N_i^{(\mathrm{p})}) + Q'_{p,N}({}^{N}z_h;\, {}^{N}N_i^{(\mathrm{p})}). \tag{D.7}$$

References

[1] R. de Boer, Theory of Porous Media, Springer-Verlag, Berlin, 2000.
[2] J.P. Carter, J.R. Booker, J.C. Small, The analysis of finite elasto-plastic consolidation, Int. J. Numer. Anal. Methods Geomech. 3 (2) (1979) 107–129.
[3] J.C. Small, J.R. Booker, E.H. Davis, Elasto-plastic consolidation of soil, Int. J. Solids Struct. 12 (6) (1976) 431–448.
[4] J.C. Small, J.R. Booker, Finite layer analysis of primary and secondary consolidation, in: Proceedings of the Fourth International Conference on Numerical Methods in Geomechanics, Vol. 1, Balkema, 1982, pp. 365–371.
[5] K. Runesson, On non-linear consolidation of soft clay (Ph.D. thesis), Department of Structural Mechanics, Chalmers University of Technology, 1978.
[6] D. Aubry, D. Lucas, B. Tie, Adaptive strategy for transient/coupled problems Application to thermoelasticity and elastodynamics, Comput. Methods Appl. Mech. Engrg. 176 (1999) 41–50.
[7] M.A. Hicks, Coupled computations for an elastic-perfectly plastic soil using adaptive mesh refinement, Int. J. Numer. Anal. Methods Geomech. 24 (2000) 453–476.
[8] K. Runesson, F. Larsson, P. Hansbo, Space–time finite elements and adaptive strategy for the coupled poroelasticity problem, in: D.W. Smith, J.P. Carter (Eds.), Proceedings of Developments in Theoretical Geomechanics, Balkema, Rotterdam, 2000, pp. 193–213.
[9] F. Larsson, P. Hansbo, K. Runesson, Space–time finite elements and an adaptive strategy for the coupled thermoelasticity problem, Internat. J. Numer. Methods Engrg. 56 (2003) 261–293.
[10] K. Eriksson, D. Estep, P. Hansbo, C. Johnson, Introduction to adaptive methods for differential equations, Acta Numer. (1995) 105–158.
[11] K. Eriksson, D. Estep, P. Hansbo, C. Johnson, Computational Differential Equations, Cambridge University Press, 1996.
[12] R. Rannacher, Error control in finite element computations: an introduction to error estimation and mesh-size adaptation, in: H. Bulgak, C. Zenger (Eds.), Error Control and Adaptivity in Scientific Computing, Kluwer Academic, 1999, pp. 247–278.
[13] P. Díez, G. Calderón, Goal-oriented error estimation for transient parabolic problems, Comput. Mech. 39 (2007) 631–646.
[14] P. Ladevèze, L. Chamoin, É. Florentin, Strict upper and lower bounds of outputs of interest for linear and nonlinear structural problems, in: P. Díez, N.E. Wiberg (Eds.), Adaptive Modeling and Simulation 2005, CIMNE, Barcelona, 2005, pp. 22–25.
[15] J. Hoffman, Adaptive simulation of the turbulent flow past a sphere, J. Fluid Mech. 568 (2006) 77–88.
[16] F. Verdugo, N. Parés, P. Díez, Goal-oriented space–time adaptivity for transient dynamics using a modal description of the adjoint solution, Comput. Mech. 54 (2014) 331–352.
[17] L. Chamoin, P. Ladevèze, Bounds on history-dependent or independent local quantities in viscoelasticity problems solved by approximate methods, Internat. J. Numer. Methods Engrg. 71 (2007) 1387–1411.
[18] N. Parés, P. Díez, A. Huerta, Bounds of functional outputs for parabolic problems. part I: exact bounds of the discontinuous Galerkin time discretization, Comput. Methods Appl. Mech. Engrg. 197 (2008) 1641–1660.
[19] N. Parés, P. Díez, A. Huerta, Bounds of functional outputs for parabolic problems. part II: bounds of the exact solution, Comput. Methods Appl. Mech. Engrg. 197 (2008) 1661–1679.
[20] J. Waeytens, L. Chamoin, P. Ladevèze, Guaranteed error bounds on pointwise quantities of interest for transient viscodynamics problems, Comput. Mech. 49 (2012) 291–307.
[21] S. Prudhomme, J.T. Oden, On goal-oriented error estimation for elliptic problems: application to the control of pointwise errors, Comput. Methods Appl. Mech. Engrg. 176 (1999) 313–331.
[22] F. Larsson, P. Hansbo, K. Runesson, Strategies for computing goal-oriented a posteriori error measures in nonlinear elasticity, Internat. J. Numer. Methods Engrg. 55 (2002) 879–894.
[23] E. Stein, M. Rüter, S. Ohnimus, Adaptive finite element analysis and modelling of solids and structures. Findings, problems and trends, Internat. J. Numer. Methods Engrg. 60 (2004) 103–138.
[24] F. Larsson, K. Runesson, P. Hansbo, Time finite elements and error computation for (visco)plasticity with hardening or softening, Internat. J. Numer. Methods Engrg. 56 (2003) 2213–2232.
[25] F. Larsson, K. Runesson, Adaptive computational meso-macro-scale modeling of elastic composites, Comput. Methods Appl. Mech. Engrg. 195 (2006) 324–338.